Original Paper

International Archives of Allergy and Immunology

Int Arch Allergy Immunol 2005;136:23–32
DOI: 10.1159/000082581

Received: April 27, 2004
Accepted after revision: September 1, 2004
Published online: December 8, 2004

Kinetic Analysis of Pepsin Digestion of Chicken Egg White Ovomucoid and Allergenic Potential of Pepsin Fragments

Kayoko Takagi[a] Reiko Teshima[a] Haruyo Okunuki[a] Satsuki Itoh[a]
Nana Kawasaki[a] Toru Kawanishi[a] Takao Hayakawa[a] Yoichi Kohno[b]
Atsuo Urisu[c] Jun-ichi Sawada[a]

[a]National Institute of Health Sciences, Tokyo; [b]Department of Pediatrics, Graduate School of Medicine, Chiba University, Chiba, and [c]Department of Pediatrics, Fujita Health University School of Medicine, Aichi, Japan

Key Words
Ovomucoid · Allergen · Digestion · Simulated gastric fluid · Fragment, pepsin-digested · Human serum IgE

Abstract
Background: The allergenic potential of chicken egg white ovomucoid (OVM) is thought to depend on its stability to heat treatment and digestion. Pepsin-digested fragments have been speculated to continue to exert an allergenic potential. OVM was digested in simulated gastric fluid (SGF) to examine the reactivity of the resulting fragments to IgE in sera from allergic patients. ***Methods:*** OVM was digested in SGF and subjected to SDS-PAGE. The detected fragments were then subjected to N-terminal sequencing and liquid chromatography/mass spectrometry/mass spectrometry analysis to confirm the cleavage sites and partial amino acid sequences. The reactivity of the fragments to IgE antibodies in serum samples from patients allergic to egg white was then determined using Western blotting (n = 24). ***Results:*** The rate of OVM digestion depended on the pepsin/OVM ratio in the SGF. OVM was first cleaved near the end of the first domain, and the resulting fragments were then further digested into smaller fragments. In the Western blot analysis, 93% of the OVM-reactive sera also bound to the 23.5- to 28.5-kDa fragments, and 21% reacted with the smaller 7- and 4.5-kDa fragments. ***Conclusion:*** When the digestion of OVM in SGF was kinetically analyzed, 21% of the examined patients retained their IgE-binding capacity to the small 4.5-kDa fragment. Patients with a positive reaction to this small peptide fragment were thought to be unlikely to outgrow their egg white allergy. The combination of SGF-digestibility studies and human IgE-binding experiments seems to be useful for the elucidation and diagnosis of the allergenic potential of OVM.

Introduction

Chicken egg white is one of the strongest and most frequent causes of food allergies among young children [1–5]. Egg white contains several allergens, including ovalbumin, ovotransferrin, lysozyme and ovomucoid (Gal d 1, OVM). OVM accounts for about 11% of all egg white proteins [6] and has a molecular weight of 28 kDa, containing a carbohydrate content of 20–25% [7]. OVM is known to be stable to digestion and heat, and cooked eggs can cause allergic reactions in OVM-specific allergic patients [8–11]. One possible reason for this is that OVM contains linear epitopes that are only slightly affected by conformational changes induced by heat denaturation.

KARGER
Fax + 41 61 306 12 34
E-Mail karger@karger.ch
www.karger.com

1018–2438/05/1361–0023$22.00/0

Accessible online at:
www.karger.com/iaa

Correspondence to: Dr. Reiko Teshima
National Institute of Health Sciences, Division of Biochemistry and Immunochemistry
1-18-1 Kamiyoga, Setagaya-ku
Tokyo 158-8501 (Japan)
Tel. +81 3 3700 1141, ext. 243, Fax +81 3 3707 6950, E-Mail rteshima@nihs.go.jp

OVM consists of 186 amino acids divided into three domains of about 60 amino acids each; the third domain has been reported to be the most important domain with regard to allergenicity [12]. In a previous report, N-glycans in the third domain were suggested to be essential for allergenicity [13]; however, a recent report found that the deletion of the N-glycans did not affect the allergic reactivity.

We previously reported the digestibility of 10 kinds of food proteins in simulated gastric fluid (SGF) [8, 14]. OVM was digested relatively rapidly, but several fragments were detected by sodium dodecyl sulfate-polyacrylamide gel electrophoresis (SDS-PAGE) followed by Coomassie blue (CBB) staining. The reactivity of these fragments with IgE antibodies from the sera of patients with egg white allergy is very important to understanding the mechanism of OVM allergy.

A few previous reports have described the reactivity of IgE in sera from patients with egg white allergies with OVM-derived fragments. Kovacs-Nolan et al. [15] separated pepsin-digested fragments of OVM using high-performance liquid chromatography (HPLC) and examined the IgE-binding activities of each fragment using an enzyme-linked immunosorbent assay (ELISA). Besler et al. [16] investigated the reactivity of pepsin-digested fragments with patient IgE using Western blotting and showed that the fragments retain their binding capacity to human IgE in some serum samples from OVM-allergic patients. However, little attention has been paid to the digestive conditions, and the number of serum samples has been somewhat small in these studies. Urisu et al. [17] reported that the sera of subjects that tested positive or negative during an oral egg white challenge exhibited a significant difference in their reactivity with pepsin fragments.

In the present report, kinetic data for different generations of SGF-stable OVM fragments were obtained, and the reactivity of the fragments with serum IgE from patients with egg white allergies was investigated using Western blotting.

Materials and Methods

Pepsin (catalog number P6887) and chicken egg white OVM (T2011, Trypsin Inhibitor, Type III-O) were purchased from Sigma Chemical Co. (St. Louis, Mo., USA). The concentration of the OVM test solution was 5 mg/ml of water. The gels and reagents used for the SDS-PAGE analysis were purchased from Invitrogen (Carlsbad, Calif., USA).

Serum Specimens

Sera from 24 patients with egg white allergies and a healthy volunteer were used after obtaining informed consent from the patients and ethical approval by the Institutional Review Board of the National Institute of Health Sciences. Twenty-two of the patients had been diagnosed as having an egg white allergy at hospitals in Japan, based on their clinical histories and positive IgE responses to egg white proteins by radioallergosorbent test (RAST), while the remaining 2 allergen-specific sera were purchased from Plasma Lab International (Everett, Wash., USA); the commercial sera originated from adult Caucasians who had been diagnosed as having several food allergies, including egg white, based on their clinical history and skin tests. The commercial sera also showed positive IgE responses to egg white proteins when examined using RAST.

Preparation of SGF

Pepsin (3.8 mg; approximately 13,148 units of activity) was dissolved in 5 ml of gastric control solution (G-con; 2 mg/ml NaCl, pH adjusted to 2.0 with distilled HCl), and the activity of each newly prepared SGF solution was defined as the production of a $\Delta A280$ of 0.001/min at pH 2.0 and 37°C, measured as the production of trichloroacetic acid-soluble products using hemoglobin as a substrate. The original SGF was prepared at a pepsin/OVM concentration of 10 unit/μg, and this solution was diluted with G-con for the experiments performed at pepsin/OVM concentrations of 1 and 0.1 unit/μg. The SGF solutions were used within the same day.

Digestion in SGF

SGF (1,520 μl) was incubated at 37°C for 2 min before the addition of 80 μl of OVM solution (5 mg/ml). The digestion was started by the addition of OVM. At each scheduled time point (0.5, 2, 5, 10, 20, 30, and 60 min), 200 μl of the reaction mixture was transferred to a sampling tube containing 70 μl of 5 × Laemmli buffer (40% glycerol, 5% 2-mercaptoethanol, 10% SDS, 0.33 *M* Tris, 0.05% bromophenol blue, pH 6.8) and 70 μl of 200 m*M* Na_2CO_3. For the zero-point samples, the OVM solution (10 μl) was added to neutralized SGF (190 μl of SGF, 70 μl of 5 × Laemmli buffer, and 70 μl of 200 m*M* Na_2CO_3). All neutralized samples were then boiled at 100°C for 3 min and subjected to SDS-PAGE.

SDS-PAGE Analysis and Staining Procedure

Samples (15 μl/lane) were loaded onto a 10–20% polyacrylamide Tris/Tricine gel (Invitrogen, Carlsbad, Calif., USA) and separated electrophoretically. The gels were fixed for 5 min in 5% trichloroacetic acid, washed for 2 h with SDS Wash (45.5% methanol, 9% acetic acid), stained for 10 min with CBB solution (0.1% Coomassie Brilliant blue R, 15% methanol, 10% acetic acid), and destained with 25% methanol and 7.5% acetic acid. The stained gel images were then analyzed using Image Gauge V3.1 (Fuji Film, Tokyo, Japan), and the density of each band was quantified. Periodic acid-Schiff (PAS) staining [18] was used to detect the glycosylated fragments.

N-Terminal Sequence Analysis

OVM (1.5 mg) was digested in SGF containing 1 unit/ml pepsin, concentrated by centrifugation using Centriprep YM-3 (Millipore Corporation, Bedford, Mass., USA) and subjected to SDS-PAGE followed by electrical transblotting to a 0.2-μm polyvinylidene difluoride membrane (Bio-Rad, Richmond, Calif., USA) and CBB staining. The detected fragment bands were then cut out and sequenced using a Procise 494HT Protein Sequencing System (Applied Biosys-

tems, Foster City, Calif., USA) or an HP G1005A Protein Sequencing System (Hewlett-Packard, Palo Alto, Calif., USA); each fragment was analyzed for 5 cycles.

Carboxymethylation and Peptide Mapping Using Liquid Chromatography/Mass Spectrometry/Mass Spectrometry (LC/MS/MS)

The digested OVM sample was separated electrophoretically as described above, stained with CBB, and the stained bands were cut out. The gel pieces were homogenized in 20 m*M* Tris-HCl (pH 8.0) containing 0.1% SDS and the proteins were extracted. The extracts were concentrated and purified by acetone precipitation. The acetone precipitates were incubated with 2-mercaptethanol (92.5 m*M*) in 72 µl of 0.5 *M* Tris-HCl buffer (pH 8.6) containing 8 *M* guanidine hydrochloride and 5 m*M* EDTA at room temperature for 2 h. To this solution, 1.5 mg of monoiodoacetic acid was added, and the mixture was incubated at room temperature for 2 h in the dark. The reaction mixture was desalted using a MicroSpin G-25 column (Amersham Bioscience, Uppsala, Sweden) and lyophilized. Reduced and carboxymethylated proteins were digested with trypsin (50 ng/µl in 50 m*M* NH_4HCO_3).

Tandem electrospray mass spectra were recorded using a hybrid quadruple/time-of-flight spectrometer (Qstar Pulsar i; Applied Biosystems, Foster City, Calif., USA) interfaced to a CapLC (Magic 2002; Michrom BioResources, Auburn, Calif., USA). Samples were dissolved in water and injected into a C18 column (0.2 × 50 mm, 3 µm, Magic C18, Michrom BioResources). Peptides were eluted with a 5–36% acetonitrile gradient in 0.1% aqueous formic acid over 60 min at a flow rate of 1 µl/min after elution with 5% acetonitrile for 10 min. The capillary voltage was set to 2,600 V, and data-dependent MS/MS acquisitions were performed using precursors with charge states of 2 and 3 over a mass range of 400–2,000.

Western Blotting of Digested Fragments with Human Serum IgE

The digested OVM samples were applied to a 10–20% polyacrylamide Tris/Tricine 2D gel, followed by electrical transfer to a nitrocellulose membrane. The membrane was then blocked with 0.5% casein-PBS (pH 7.0) and cut into 4-mm strips. The strips were incubated with diluted human serum (1/4 to 1/5) in 0.2% casein-PBS (pH 7.0) at room temperature for 1 h and then at 4°C for 18 h. After washing with 0.05% Tween 20-PBS, the strips were incubated with rabbit anti-human IgE (Fc) antibodies (Nordic Immunological Laboratories, Tilburg, The Netherlands) at room temperature for 1 h, and then with horseradish peroxidase-conjugated donkey anti-rabbit Ig antibodies (Amersham Biosciences, Little Chalfont, UK) at room temperature for 1 h. Finally, the strips were reacted with Konica ImmunoStain HRP-1000 (Konica, Tokyo, Japan), according to the manufacturer's protocol.

Results

Kinetics of OVM Digestion by Pepsin

OVM was digested in SGF containing various concentrations of pepsin, and the fragments were separated by SDS-PAGE and stained with CBB (fig. 1). The molecular weight of OVM, based on its amino acid sequence, is about 20 kDa, but a broad band representing intact OVM appeared at about 34–49 kDa in the SDS-PAGE gel because of the presence of five N-linked sugar chains. The pepsin band was detected at 39 kDa, overlapping with the intact OVM band, and lysozyme (14 kDa) contamination was detected in the OVM sample that was used. Intact OVM rapidly disappeared within 0.5 min in SGF (pepsin/OVM = 10 unit/µg), and a fragment band was detected at 7 kDa. When the pepsin content in SGF was reduced to 1 and 0.1 unit/µg, the digestion rate markedly decreased. Intact OVM was still detected after 30 min when the pepsin/OVM ratio was 0.1 unit/µg. The fragment bands were clearer (fig. 2) when a concentrated SGF-digested OVM solution (pepsin/OVM = 1 unit/µg, digestion times 5 and 30 min) was used, followed by SDS-PAGE. As shown in figure 2, a strong 23.5- to 28.5-kDa band (FR 1) was detected at 5 min, while 10- (FR 2), 7- (FR 3) and 4.5- to 6-kDa (FR 4) bands were detected after 30 min. FR 1 and FR 2 were both positively stained by PAS, suggesting that the FR 1 and FR 2 fragments have high carbohydrate contents. The time courses for the amounts of intact OVM and the four fractions are plotted in figure 3, where the pepsin/OVM ratio is 1 unit/µg. FR 1 rapidly increased but slowly disappeared after 2 min. FR 2 and FR 3 also rapidly reached maximum values at 5 min and then slowly disappeared. On the other hand, FR 4 gradually increased throughout the entire period of the experiment.

Preheating (at 100°C for 5 or 30 min) of the OVM solution (5 mg/ml in water) did not influence the digestion pattern (fig. 1).

Table 1. N-Terminal sequences of pepsin fragments

Digestion period	Fraction	Fragment	Residues	Sequence	Ratio %[a]
5 min	FR 1	1-1	50–54	FGTNI	73.1
		1-2	51–55	GTNIS	11.6
		1-3	1–5	AEVDC	6.9
5 min	FR 2	2-1	1–5	AEVDC	68.8
		2-2	134–138	VSVDC	28.2
5 min	FR 3	3-1	1–5	AEVDC	48.4
		3-2	134–138	VSVDC	24.3
		3-3	104–108	NECLL	9.6
		3-4	85–89	VLCNR	6.5
30 min	FR 4	4-1	134–138	VSVDC	30.6
		4-2	104–108	NECLL	24.0
		4-3	19–23	VLVCN	20.6

[a] Molar ratios of the fragments to the total amount in each fraction.

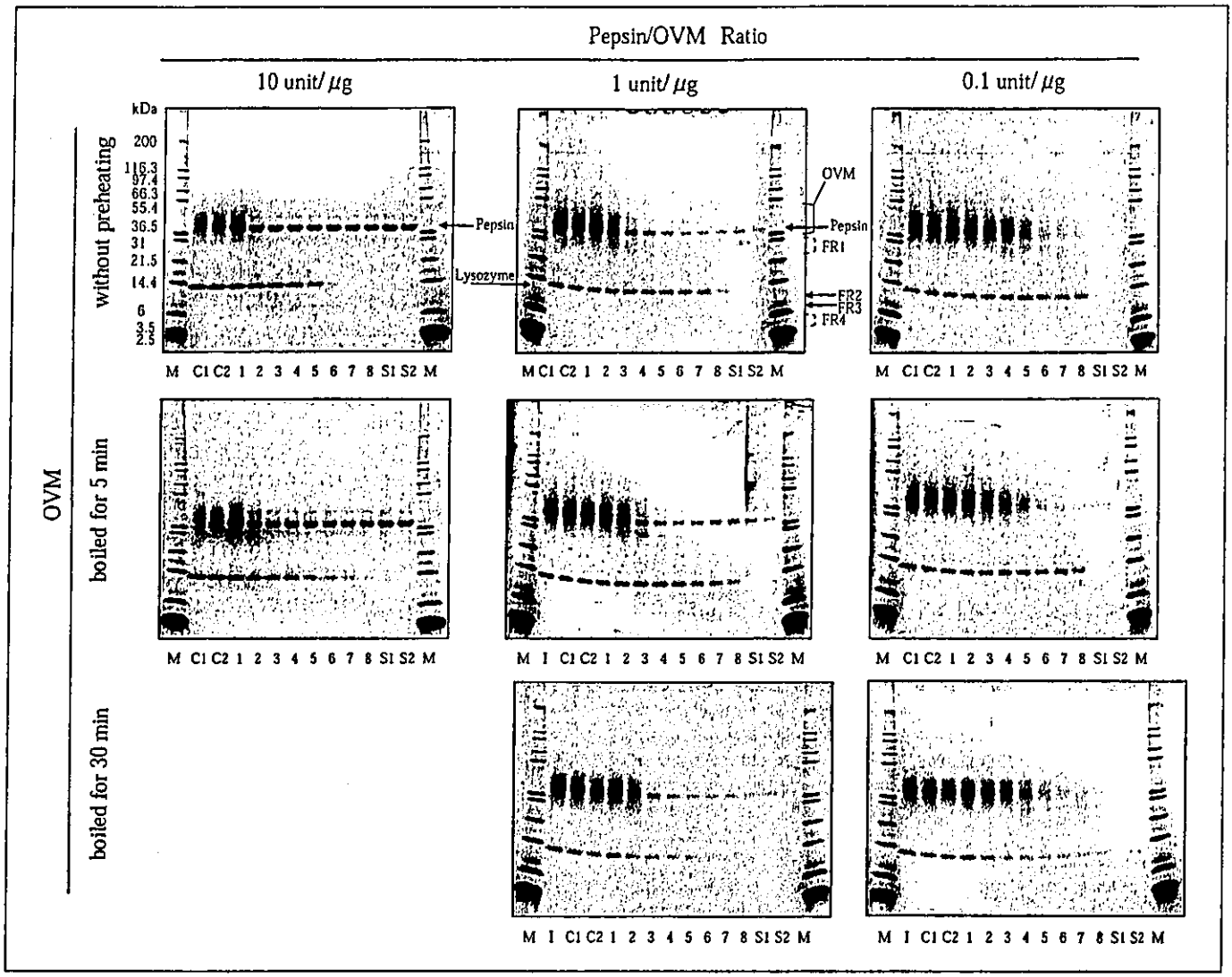

Fig. 1. Kinetic patterns of OVM digestion in SGF-containing pepsin. Digested samples were analyzed by SDS-PAGE followed by CBB staining. The digestion patterns of OVM without preheating (upper panels), preheated at 100°C for 5 min (middle panels), and preheated at 100°C for 30 min (lower panels) are shown. The ratio of pepsin to OVM was 10 unit/1 μg (left), 1 unit/1 μg (middle), and 0.1 unit/1 μg (right). Lane M = Molecular weight markers; lanes C1 and C2 = OVM without pepsin at 0 (C1) and 60 (C2) min; lanes 1–8 = SGF-digested OVM at 0, 0.5, 2, 5, 10, 20, 30 and 60 min, respectively; lanes S1 and S2 = SGF alone at 0 (S1) and 60 (S2) min; lanes I = OVM without preheating; FR 1 = fraction 1 containing a fragment at 23.5–28.5 kDa; FR 2 = fraction 2 containing a 10-kDa fragment; FR 3 = fraction 3 containing a 7-kDa fragment; FR 4 = fraction 4 containing 4.5- to 6-kDa fragments.

Sequence Analysis of OVM Fragments

The sequences of the five N-terminal residues in each fragment were analyzed, and the data are summarized in table 1. Figure 4 schematically depicts the identified fragments; the arrows in the upper panel indicate the sites of pepsin cleavage.

The internal sequences of the FR 1, FR 3, and FR 4 fragments were also identified by LC/MS/MS and are shown in table 2 and in the upper panel of figure 4.

Reactivity of the Fragments with Serum IgE from Patients with Egg White Allergy

Western blot analysis using patient sera as the source of the primary antibodies was performed to identify sera that reacted with intact OVM and the SGF fragments. Representative blotting data are shown in figure 5, and all the results are listed in table 3. Ninety-two percent of the serum samples from allergic patients reacted with OVM, and 93% of the OVM-positive sera reacted with FR 1

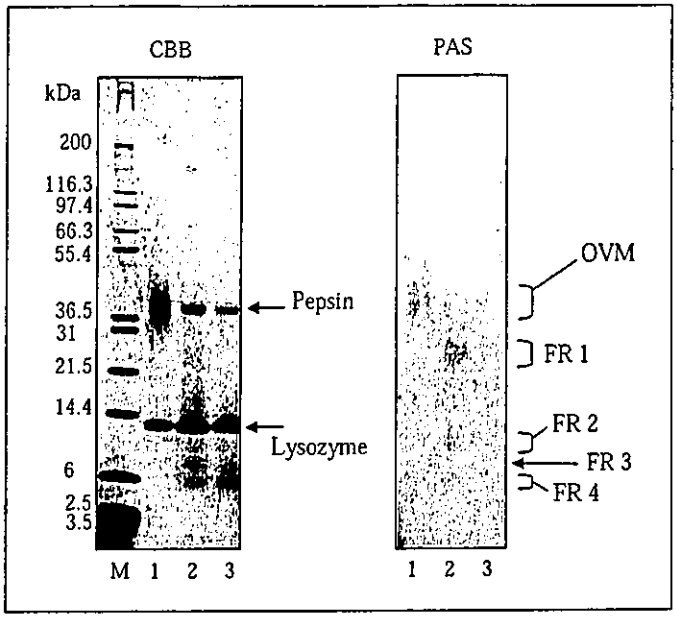

Fig. 2. CBB and PAS staining of OVM fragments following digestion in SGF (pepsin/OVM = 1 unit/μg) for 5 and 30 min. Lane M = Molecular weight markers; lane 1 = original OVM (2.5 μg/lane); lanes 2 and 3 = OVM digested for 5 and 30 min, respectively, and concentrated (12 μg, equivalent to the original OVM/lane). Samples were applied to two SDS-PAGE gels and electrophoresed. One plate (left panel) was stained with CBB reagent, and the other (right panel) was stained with PAS reagent.

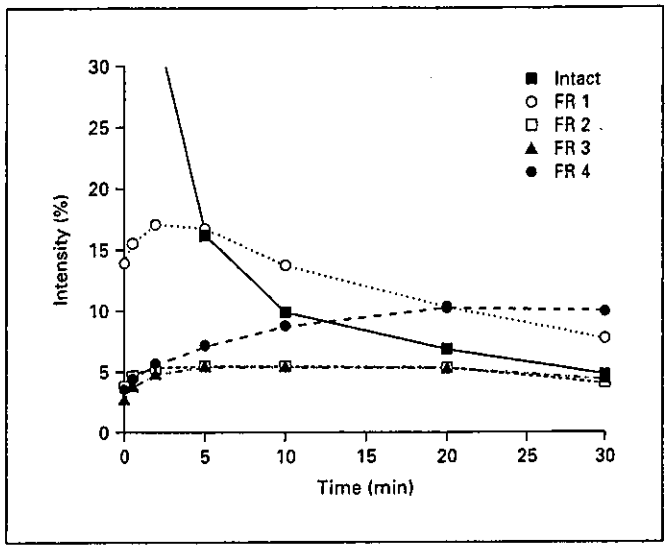

Fig. 3. Quantification of the SGF-digestion pattern of intact OVM and the digestion fragments at a pepsin/OVM ratio of 1 unit/μg. The intensity of each band was calculated using the ratio of the band's density to the total density of the originally detected band at t = 0. Values are the mean of duplicate analyses. Similar results were observed in another set of experiments.

Table 2. Identified inside sequences in pepsin- and trypsin-digested OVM

Pepsin digestion	Fraction	Residues	Sequence
5 min	FR 1	83–89	VMVLCNR
		90–103	AFNPVCGTDGVTYD
		90–112	AFNPVCGTDGVTYDNECLLCAHK
		90–122	AFNPVCGTDGVTYDNECLLCAHKVEQGASVDKR
		113–122	VEQGASVDKR
5 min	FR 3	90–112	AFNPVCGTDGVTYDNECLLCAHK
		90–122	AFNPVCGTDGVTYDNECLLCAHKVEQGASVDKR
		104–111	NECLLCAH
		104–112	NECLLCAHK
		104–121	NECLLCAHKVEQGASVDK
		104–122	NECLLCAHKVEQGASVDKR
		113–122	VEQGASVDKR
		134–159	VSVDCSEYPKPDCTAEDRPLCGSDNK
		165–185	CNFCNAVVESNGTLTLSHFGK
30 min	FR 4	90–112	AFNPVCGTDGVTYDNECLLCAHK
		104–111	NECLLCAH
		104–112	NECLLCAHK
		104–122	NECLLCAHKVEQGASVDKR
		112–122	KVEQGASVDKR
		113–121	VEQGASVDK
		113–122	VEQGASVDKR
		165–185	CNFCNAVVESNGTLTLSHFGK

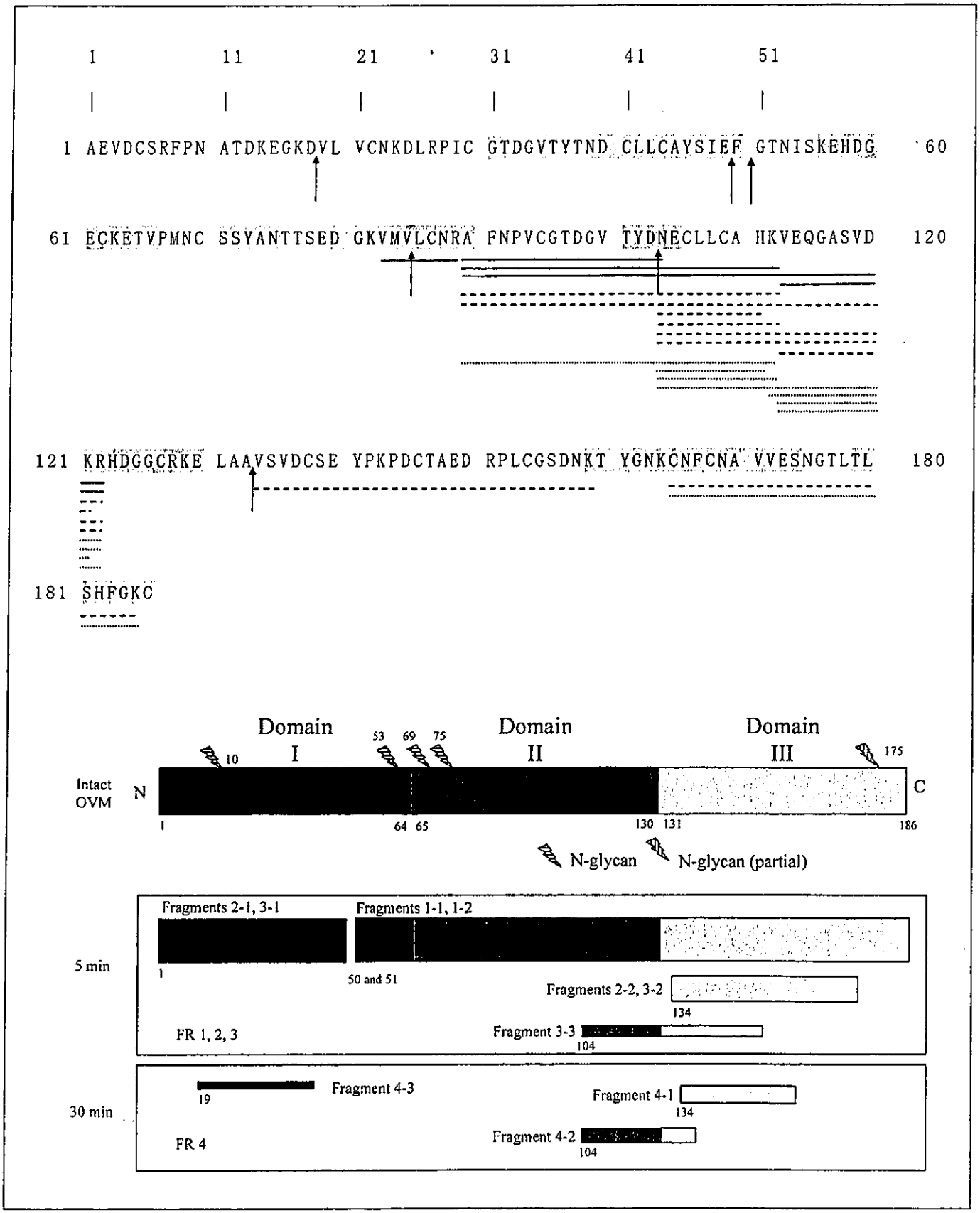
1 11 21 31 41 51
1 AEVDCSRFPN ATDKEGKDVL VCNKDLRPIC GTDGVTYTND CLLCAYSIEF GTNISKEHDG 60
61 ECKETVPMNC SSYANTTSED GKVMVLCNRA FNPVCGTDGV TYDNECLLCA HKVEQGASVD 120
121 KRHDGGCRKE LAAVSVDCSE YPKPDCTAED RPLCGSDNKT YGNKCNFCNA VVESNGTLTL 180
181 SHFGKC
Domain I
Domain II
Domain III
10
53
69
75
175
Intact OVM
N
C
1
64 65
130 131
186
N-glycan
N-glycan (partial)
5 min
Fragments 2-1, 3-1
Fragments 1-1, 1-2
1
50 and 51
Fragments 2-2, 3-2
134
FR 1, 2, 3
Fragment 3-3
104
30 min
19
Fragment 4-3
Fragment 4-1
134
FR 4
Fragment 4-2
104

4

after 5 min of digestion. Three of the serum samples also reacted with FR 2, FR 3, and FR 4 after 30 min of digestion.

The three samples that react with FR 2, FR 3, and FR 4 were obtained from patients who exhibited persistent allergies to egg white. One of these serum samples, No.4, was obtained from a 3-year-old girl who is presently 6 years old; her total IgE level has decreased slightly to 4,450 IU/ml, but the specific IgE level for egg white remains at more than 100 IU/ml, and the patient has not outgrown her hypersensitivity to eggs. Another patient, No. 13, was a 1-year-old boy; 7 years later, his total and egg white-specific IgE levels had been reduced to 947 and 6.85 IU/ml, respectively, but eating raw eggs still caused allergic symptoms. The third FR 4-positive patient, No. 19, was an 11-year-old boy whose total IgE level decreased to 3,940 IU/ml and whose egg white-specific IgE decreased to 13.5 IU/ml after a period of about 2 years; however, this patient has also not outgrown his allergies. These cases and our previously reported data [17] indicate that the induction of egg white tolerance may be difficult in patients whose serum IgE exhibits binding activity to digested small fragments of OVM.

Discussion

In the SGF-digestion system, preheating the OVM (100°C for 5 or 30 min) did not affect the OVM digestion pattern (fig. 1), consistent with the results of previous reports [9] in which heat treatment did not markedly decrease the allergenicity of OVM. On the other hand, a decrease in the pepsin/OVM ratio dramatically reduced the digestion rate, suggesting that digestibility may vary depending on the amount of OVM intake and the conditions of the individual's digestion system. In its native state, OVM possesses serine protease inhibitor activity. Fu et al. [11] and our group [10] previously reported that intact OVM was stable for 60 min in simulated intestinal fluid. Kovacs-Nolan et al. [15] also reported that pepsin-

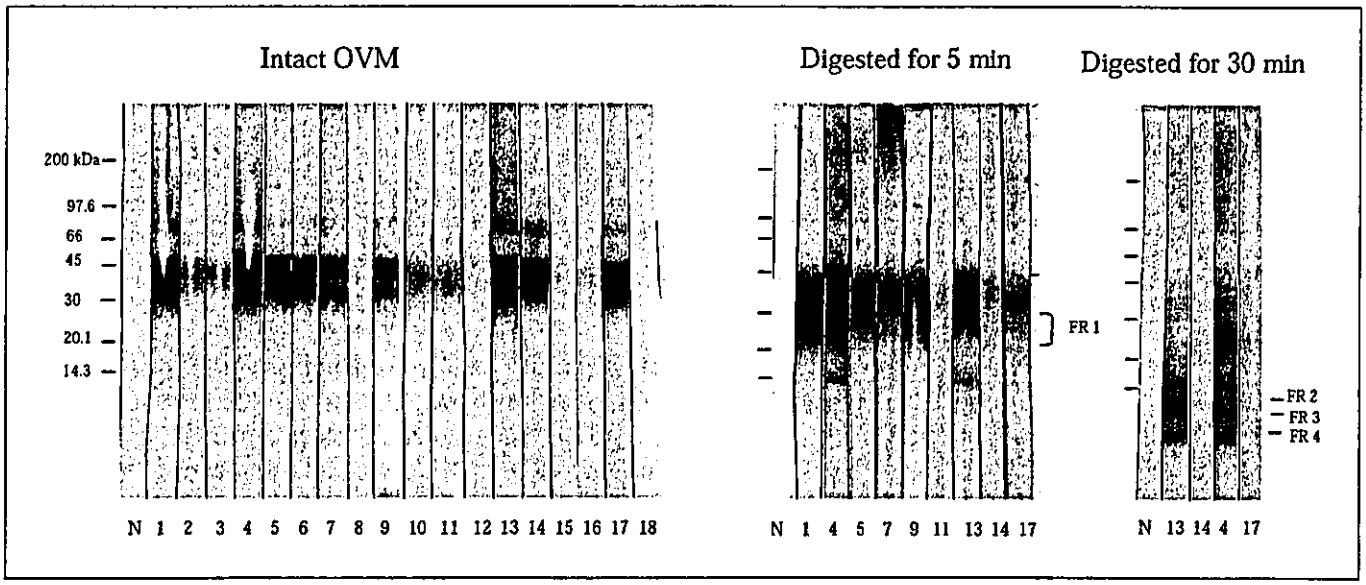

Fig. 4. Amino acid sequence and schematic representation of the SGF-digestion pattern of OVM. The amino acid sequence of OVM is shown in the upper panel. The arrows indicate the SGF-digested points according to the results of an N-terminal analysis of the OVM fragments (table 1), and the underlined regions indicate sequences identified by LC/MS/MS. Solid line = FR 1; dotted line = FR 3; dashed line = FR 4. Shaded areas represent reported human IgE epitopes [16]. The lower panel is a summary of the OVM digestion pattern according to N-terminal analysis.

Fig. 5. Western blot analysis of intact OVM and the fragments with serum IgE from egg white allergic patients and a normal volunteer. The fragments were prepared as described in the legend of figure 2. The number of each strip corresponds to the sample numbers in table 2.

Table 3. Reactivity of OVM and pepsin fragments with patient serum IgE

No.	IgE content, IU/ml		Reactivity with patient IgE[1]				
	total	egg white-specific	intact OVM	FR 1	FR 2	FR 3	FR 4
1	3,700	>100	+++	++	–	–	–
2	402	3.74	+	n.d.	n.d.	n.d.	n.d.
3	251	6.85	+	n.d.	n.d.	n.d.	n.d.
4	6,510	>100	+++	+++	+	+	++
5	2,060	>100	++	++	–	–	–
6	1,240	12.4	++	n.d.	n.d.	n.d.	n.d.
7	4,180	31.3	++	++	–	–	–
8	56	20.1	±	n.d.	n.d.	n.d.	n.d.
9	1,355	50.7	++	++	–	–	–
10	22,810	2.11	+	n.d.	n.d.	n.d.	n.d.
11	1,463	4.65	+	–	–	–	–
12	14,230	0.70–3.49	±	n.d.	n.d.	n.d.	n.d.
13	8,000	>100	+++	+++	+	+	++
14	22,490	1.05	+++	±	–	–	–
15	934	66.3	+	n.d.	n.d.	n.d.	n.d.
16	345	20.1	+	n.d.	n.d.	n.d.	n.d.
17	1,500	80	++	+	–	–	–
18	3,300	>10	–	n.d.	n.d.	n.d.	n.d.
19	20,500	26.8	+++	++	±	±	±
20	138	45.4	++	+	–	–	–
21	940	2.44	+	+	–	–	–
22	91	0.70–3.49	+	±	–	–	–
23	828	0.9	++	+	–	–	–
24	21	3.50–17.4	–	n.d.	n.d.	n.d.	n.d.
	positive/tested		22/24 (92%)[2]	13/14 (93%)[3]	3/14 (21%)[3]	3/14 (21%)[3]	3/14 (21%)[3]

n.d. = Not done.

[1] Intensity of the reactivity of each band was evaluated by the ratio to normal serum: – = <1; ± = 1–2; + = 2–5; ++ = 5–10; +++ = >10.

[2] Percent of egg white-positive samples.

[3] Percent of intact OVM-positive samples.

digested OVM retains its trypsin inhibitor activity. Therefore, OVM and its pepsin-digested fragments were thought to be stable in the small intestine.

At a pepsin/OVM ratio of 1 unit/μg, FR 1 reached a maximum level after 2 min of digestion, while both FR 2 and FR 3 reached maximum levels after 5 min of digestion; thereafter, FR 1, FR 2, and FR 3 gradually decreased. However, FR 4 increased continuously throughout the 30-min period of digestion and the major fragments were seen after 30 min of digestion (fig. 3). FR 4 was mainly composed of three fragments whose N-terminals were 134V, 104N and 19V (table 1). A C-terminal sequence, 165N–185C, was also identified in FR 4 (table 2). These fragments contain known IgE epitopes [19] and therefore may cause allergic responses. Three of the OVM-positive sera from patients with egg white allergy reacted positively with the FR 4 fragments (table 3).

The present results are consistent with the previous finding that pediatric subjects with a higher IgE-binding activity to pepsin-treated OVM were unlikely to outgrow their egg allergy [17]. For peanut allergies, differences in IgE-binding epitopes have been reported between the patients with clinically active peanut allergies and those who developed a tolerance, regardless of the presence of high or low peanut-specific IgE levels [20].

The N-terminal residue of the major fragment (4-1) of FR 4 was Val-134 (30%; table 1). This fragment retains most of domain III, which has been reported to have significantly higher human IgG- and IgE-binding activities than those of domains I and II [12]. A domain-III OVM

variant has also been reported to cause a reduction in immunogenicity and allergenicity [21].

Domains I, II, and III contain one, three, and one N-glycosylation sites, respectively [7]. The possible relation between the carbohydrate chain in domain III and allergenicity is interesting. One report suggested that this carbohydrate chain may play an important role in allergenic determinants against human IgE antibody [13], and another report suggested that the carbohydrate chains of OVM may protect against peptic hydrolysis [22]. However, the carbohydrate moieties have been shown to have only a minor effect on allergenicity [23]. As shown in figure 2, intact OVM, FR 1, and FR 2 fragments were detected using PAS staining, suggesting the presence of carbohydrate chains, but FR 4 was not stained with the PAS reagent, despite being clearly detected with CBB. Therefore, FR 4 might contain little or no carbohydrate chains. Since FR 4 seems to maintain its allergenic potential, as described above, the absence of the carbohydrate chains in FR 4 suggests that they are not necessary for OVM allergenicity. Since the minimum peptide size capable of eliciting significant clinical symptoms of allergic reactions is thought to be 3.1 kDa [24], FR 4 may be able to trigger mast cell activation and elicit clinical symptoms.

In this report, the SGF-digestion kinetic pattern of OVM was investigated in detail, and the partial sequences of the fragments in the 4 fractions separated by SDS-PAGE were determined. Furthermore, the reactivity of the fragments with a number of serum samples from patients with egg white allergies was detected using Western blotting. The four fractions were separated according to their molecular weight and consisted of more than one fragment, as determined by N-terminal analysis. The identified sequences that started at Asn-104 and Val-134 in FR 3, as determined using LC/MS/MS (table 2), coincided with the 3-2 and 3-3 fragments in the N-terminal analysis (table 1), and the sequence that started at Asn-104 in FR 4 coincided with fragment 4-2. Moreover, the LC/MS/MS analysis indicated that FR 3 and FR 4 contained other parts of domain II and the C-terminal sequence N165–C185, which are thought to be minor components of these fractions. The combination of SGF digestion and patient IgE may provide useful information for the diagnosis and prediction of potential OVM allergenicity.

Acknowledgement

This study was supported by a grant from the Ministry of Health, Labor and Welfare, and the Cooperative System for Supporting Priority Research of Japan Science and Technology Agency.

References

1 Sampson HA, McCaskill CC: Food hypersensitivity and atopic dermatitis: Evaluation of 113 patients. J Pediatr 1985;107:669–675.

2 Bock SA, Sampson HA, Atkins FM, Zeiger RS, Lehrer S, Sachs M, Bush RK, Metcalfe DD: Double-blind, placebo-controlled food challenge (DBPCFC) as an office procedure: A manual. J Allergy Clin Immunol 1988;82:986–997.

3 Bock SA, Atkins FM: Patterns of food hypersensitivity during sixteen years of double-blind, placebo-controlled food challenges. J Pediatr 1990;117:561–567.

4 Boyano-Martinez T, Garcia-Ara C, Diaz-Pena JM, Martin-Esteban M: Prediction of tolerance on the basis of quantification of egg white-specific IgE antibodies in children with egg allergy. J Allergy Clin Immunol 2002;110:304–309.

5 Kotaniemi-Syrjanen A, Reijonen TM, Romppanen J, Korhonen K, Savolainen K, Korppi M: Allergen-specific immunoglobulin E antibodies in wheezing infants: The risk for asthma in later childhood. Pediatrics 2003;111:e255–e261.

6 Li-Chan E, Nakai S: Biochemical basis for the properties of egg white. Crit Rev Poultry Biol 1989;2:21–58.

7 Kato I, Schrode J, William J. Kohr WJ, Laskowski M Jr: Chicken ovomucoid: Determination of its amino acid sequence, determination of the trypsin reactive site, and preparation of all three of its domains. Biochemistry 1987;26:193–201.

8 Matsuda T, Watanabe K, Nakamura R: Immunochemical and physical properties of peptic-digested ovomucoid. J Agric Food Chem 1983;31:942–946.

9 Honma K, Aoyagi M, Saito K, Nishimuta T, Sugimoto K, Tsunoo H, Niimi H, Kohno Y: Antigenic determinants on ovalbumin and ovomucoid: Comparison of the specificity of IgG and IgE antibodies. Arerugi 1991;40:1167–1175.

10 Takagi K, Teshima R, Okunuki H, Sawada J: Comparative study of in vitro digestibility of food proteins and effect of preheating on the digestion. Biol Pharm Bull 2003;26:969–973.

11 Fu TJ, Abbott UR, Hatzos C: Digestibility of food allergens and nonallergenic proteins in simulated gastric fluid and simulated intestinal fluid-a comparative study. J Agric Food Chem 2002;50:7154–7160.

12 Zhang JW, Mine Y: Characterization of IgE and IgG epitopes on ovomucoid using egg-white-allergic patients' sera. Biochem Biophys Res Commun 1998;253:124–127.

13 Matsuda T, Nakamura R, Nakashima I, Hasegawa Y, Shimokata K: Human IgE antibody to the carbohydrate-containing third domain of chicken ovomucoid. Biochem Biophys Res Commun 1985;129:505–510.

14 Thomas K, Aalbers M, Bannon GA, Bartels M, Dearman RJ, Esdaile DJ, Fu TJ, Glatt CM, Hadfield N, Hatzos C, Hefle SL, Heylings JR, Goodman RE, Henry B, Herouet C, Holsapple M, Ladics GS, Landry TD, MacIntosh SC, Rice EA, Privalle LS, Steiner HY, Teshima R, Van Ree R, Woolhiser M, Zawodny J: A multi-laboratory evaluation of a common in vitro pepsin digestion assay protocol used in assessing the safety of novel proteins. Regul Toxicol Pharmacol 2004;39:87–98.

15 Kovacs-Nolan J, Zhang JW, Hayakawa S, Mine Y: Immunochemical and structural analysis of pepsin-digested egg white ovomucoid. J Agric Food Chem 2000;48:6261–6266.
16 Besler M, Petersen A, Steinhart H, Paschke A: Identification of IgE-Binding Peptides Derived from Chemical and Enzymatic Cleavage of Ovomucoid (Gal d 1). Internet Symposium on Food Allergens 1999;1:1–12. http://www.food-allergens.de
17 Urisu A, Yamada K, Tokuda R, Ando H, Wada E, Kondo Y, Morita Y: Clinical significance of IgE-binding activity to enzymatic digests of ovomucoid in the diagnosis and the prediction of the outgrowing of egg white hypersensitivity. Int Arch Allergy Immunol 1999; 120:192–198.
18 Zacharius RM, Zell TE, Morrison JH, Woodlock JJ: Glycoprotein staining following electrophoresis on acrylamide gels. Anal Biochem 1969;30:148–152.
19 Mine Y, Zhang JW: Identification and fine mapping of IgG and IgE epitopes in ovomucoid. Biochem Biophys Res Commun 2002; 292:1070–1074.
20 Beyer K, Ellman-Grunther L, Jarvinen KM, Wood RA, Hourihane J, Sampson HA: Measurement of peptide-specific IgE as an additional tool in identifying patients with clinical reactivity to peanuts. J Allergy Clin Immunol 2003;112:202–207.
21 Mine Y, Sasaki E, Zhang JW: Reduction of antigenicity and allergenicity of genetically modified egg white allergen, ovomucoid third domain. Biochem Biophys Res Commun 2003; 302:133–137.
22 Matsuda T, Gu J, Tsuruta K, Nakamura R: Immunoreactive glycopeptides separated from peptic hydrolysate of chicken egg white ovomucoid. J Food Sci 1985;50:592–594.
23 Cooke SK, Sampson HA: Allergenic properties of ovomucoid in man. J Immunol 1997;159: 2026–2032.
24 Kane PM, Holowka D, Baird B: Cross-linking of IgE receptor complexes by rigid bivalent antigens greater than 200 Å in length triggers cellular degranulation. J Cell Biol 1988;107: 969–980.

RAPID COMMUNICATIONS IN MASS SPECTROMETRY
Rapid Commun. Mass Spectrom. 2004; 18: 1156–1160
Published online in Wiley InterScience (www.interscience.wiley.com). DOI: 10.1002/rcm.1465

RCM

Improved sensitivity for insulin in matrix-assisted laser desorption/ionization time-of-flight mass spectrometry by premixing α-cyano-4-hydroxycinnamic acid matrix with transferrin

Tetsu Kobayashi*, Hiroshi Kawai, Takuo Suzuki, Toru Kawanishi and Takao Hayakawa
Division of Biological Chemistry and Biologicals, National Institute of Health Sciences, 1-18-1 Kamiyoga, Setagaya-ku, Tokyo 158-8501, Japan

Received 27 February 2004; Revised 25 March 2004; Accepted 25 March 2004

This report describes an enhancement of the signal intensities of proteins and peptides in matrix-assisted laser desorption/ionization time-of-flight mass spectrometry (MALDI-TOFMS). When α-cyano-4-hydroxycinnamic acid (CHCA) premixed with human transferrin (Tf) was used as a matrix, the signal intensity of insulin was amplified to more than ten times that of the respective control in CHCA without Tf. The detection limit of insulin was 0.39 fmol on-probe in the presence of Tf, while it was 6.3 fmol in the absence of Tf. The signal intensity of insulin was also enhanced when the CHCA matrix was premixed with proteins other than Tf (80 kDa), such as horse ferritin (20 kDa), bovine serum albumin (BSA, 66 kDa), or human immunoglobulin G (150 kDa). The optimum spectrum of insulin was obtained when the added amount of protein was in the range 0.26–0.62 pmol, regardless of the molecular weight of the added protein. Tf and BSA outperformed the other tested proteins, as determined by improvements in the resulting spectra. When the mass spectra of several peptides and proteins were recorded in the presence of Tf or BSA, the signal intensities of large peptides such as glucagon were enhanced, though those of smaller peptides were not enhanced. In addition, the signal enhancement achieved with Tf and BSA was more pronounced for the proteins, including cytochrome C, than for the large peptides. This enhancement effect could be applied to improve the sensitivity of MALDI-TOFMS to large peptides and proteins. Copyright © 2004 John Wiley & Sons, Ltd.

Matrix-assisted laser desorption/ionization time-of-flight mass spectrometry (MALDI-TOFMS) and electrospray ionization mass spectrometry have been widely used in studies of protein chemistry, including proteomics studies aimed at sequence identification or quantitative analyses following enzymatic digestion by isotope-coded affinity tags and other tagging systems.[1–8] In particular, MALDI-TOFMS has been used for the qualitative and quantitative analysis of intact proteins.[9–11] When the MALDI technique was first introduced as an ionization method for proteins, a mixture of fine metal powder and glycerol, or nicotinic acid, was used as the matrix.[12,13] Progress has been made with other matrix materials such as sinapinic acid, 2,5-dihydroxybenzoic acid (DHB), and α-cyano 4-hydroxycinnamic acid (CHCA), which have some desirable properties such as less intense adduct peaks and a relative insensitivity to contamination.[14–16] With the MALDI approach, analyte proteins are dispersed on a surface in a thin layer of matrix. The energy of an incident pulse of laser photons is absorbed by the matrix to form a jet of matrix vapor that lifts the analyte proteins from the surface and transforms some of them into ions.[13]

However, the mechanisms by which laser light irradiation is able to generate macromolecular ions have not been fully verified to date. It has been reported that the ionization of macromolecules by the MALDI process is affected by several factors. For example, peptide signal intensity was increased by the use of acetone as the solvent for CHCA matrix instead of employing the commonly used solvent, a mixture of acetonitrile and aqueous 0.1% trifluoroacetic acid (TFA).[17] The signal-to-noise (S/N) ratios for macromolecules are low in DHB matrix, but the addition of suitable additives (fructose, glucose, fucose, or 2-hydroxy-5-methoxybenzoic acid) to the DHB matrix improved its performance in the high molecular mass range.[18–21] In the CHCA and sinapinic acid matrices, the detection of higher molecular weight proteins was improved by using polytetrafluoroethylene (Teflon) as sample support.[22,23]

Recently, we investigated a method of identifying and quantifying proteins in blood using mass spectrometry. During the present study, we discovered that the signal intensity of human insulin was augmented more than 10-fold when transferrin (Tf) was mixed with the CHCA matrix

**Correspondence to*: T. Kobayashi, Division of Biological Chemistry and Biologicals, National Institute of Health Sciences, 1-18-1 Kamiyoga, Setagaya-ku, Tokyo 158-8501, Japan.
E-mail: kobayash@nihs.go.jp
Contract/grant sponsor: Ministry of Health, Labor and Welfare, Japan.

solution used for MALDI-TOFMS. This phenomenon was not specific to either insulin or Tf, which suggested that such enhancements could be used more generally to improve the sensitivity of protein analysis with MALDI-TOFMS.

EXPERIMENTAL

Materials

Human atrial natriuretic peptide (hANP), glucagon, insulin, insulin-like growth factor-1 (IGF-1), transferrin (Tf), bovine serum albumin (BSA), horse spleen ferritin (106 mg/mL in 0.15 M NaCl), and ProteoMass Peptide & Protein, were purchased from Sigma (St. Louis, MO, USA). Human immunoglobulin G (IgG, 11.3 mg/mL in 0.01 M sodium phosphate, 0.5 M NaCl, pH 7.6) was obtained from Wako Pure Chemical Industries Ltd. (Tokyo, Japan). Human insulin, IGF-1, glucagon, and hANP stock solutions were prepared at concentrations of 100 pmol/μL by dissolving them in 0.1% TFA. Tf and BSA stock solutions were prepared at concentrations of 10 mg/mL by dissolving the materials in Millipore deionized water. ProteoMass Peptide & Protein stock solutions, which include bradykinin fragment 1-7, human angiotensin II, synthetic peptide $P_{14}R$, human ACTH fragment 18-39, bovine insulin oxidized B chain, bovine insulin, equine cytochrome C, equine apomyoglobin, rabbit aldolase, and BSA, were prepared at concentrations of 100 pmol/μL each, according to the manufacturer's instructions.

Sample application and data acquisition

The Tf-mixed CHCA was a 5:1 mixture of the CHCA solution (10 mg/mL in 50% acetonitrile in 0.1% aqueous TFA) and Tf solution (0.10 μg/μL; the final concentration was approximately 8.3 ng/μL), corresponding to 0.21 pmol Tf on each well of the target plate, if not otherwise noted. The control CHCA was a mixture of the CHCA solution and deionized water (5:1). A portion of each sample solution was immediately mixed with an equal volume of the matrix solution with or without Tf, and an aliquot of 2 μL (corresponding to 1 μL of sample solution) was applied to a stainless steel target plate. Mass spectrometric analyses were performed using an AB4700 proteomics analyzer (Applied Biosystems, Foster, CA, USA). The operating conditions were as follows: Nd:YAG laser (355 nm), linear mode, and detection of positive ions. The spectra were generated by signal averaging 50 laser shots into a single spectrum. The signal intensity was obtained after performing background correction and noise reduction using the Data Processor software (Applied Biosystems). This software was also used to determine the detection limit.

To confirm whether or not the matrix solution was at an optimum composition, serially diluted CHCA, DHB, or sinapinic acid solutions (from 10 to 0.078 mg/mL in 50% acetonitrile, 50% 0.1% TFA) were added to the insulin solution (100 fmol/μL). The most intense signal was obtained when 10 mg/mL CHCA was added to the insulin solution.

RESULTS AND DISCUSSION

Human insulin solution (6.3 fmol/μL) was mixed with an equal volume of Tf-mixed CHCA or control CHCA. When

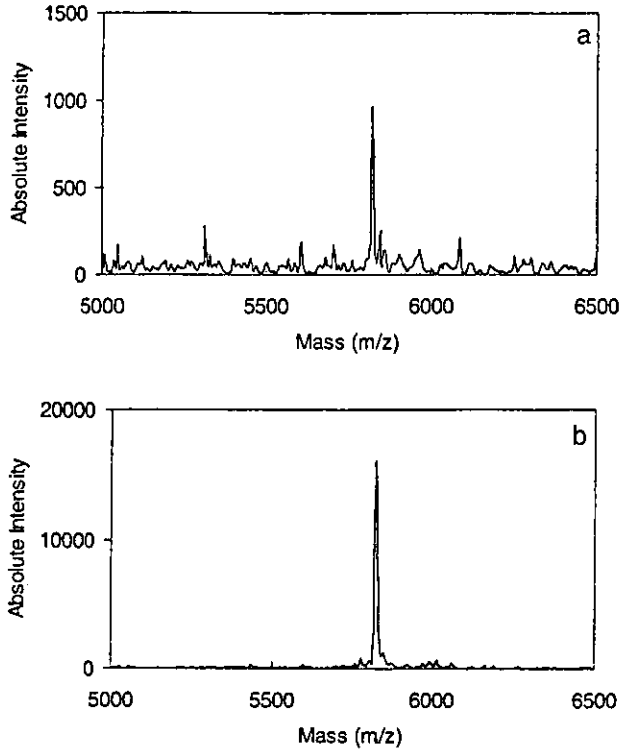

Figure 1. MALDI mass spectra of human insulin. The insulin solution (6.3 fmol/μL) and matrix solution were mixed together in equal volumes; 2 μL of the resulting mixture were applied to a target plate, allowed to dry, and analyzed by MALDI-TOFMS (see Experimental). The matrix solution was a 5:1 mixture of CHCA solution (10 mg/mL in 50% acetonitrile in 0.1% aqueous TFA) with deionized water or Tf solution (0.10 μg/μL). (a) Control CHCA used as matrix. (b) Tf-mixed CHCA used as matrix.

the Tf-mixed CHCA was used as matrix, the signal intensity of insulin in the MALDI-TOFMS detection system was amplified more than 10-fold relative to that achieved with the control CHCA (Fig. 1). To assess the sensitivity of insulin detection, the matrix solution was added to serially diluted insulin solutions (from 100 to 0.20 fmol/μL in deionized water), and samples were then spotted on a target plate. The detection limit of insulin was 0.39 fmol on the target plate in a Tf-mixed CHCA matrix under the present experimental conditions, whereas this limit was 6.3 fmol in the case of CHCA without Tf (Fig. 2).

To obtain the optimum concentration of Tf for the enhancement of insulin measurement sensitivity, the CHCA solution was mixed with serially diluted Tf solutions (from 1.0 μg/μL to 7.8 ng/μL) before addition to the insulin solution (100 fmol/μL). The signal intensity increased in a Tf-concentration-dependent manner (Fig. 3(a)). However, the S/N ratio decreased when the Tf concentration was more than 125 ng/μL (Fig. 3(b)), though it should be noted that the S/N value was still higher than the corresponding control value, i.e., 15 ± 7. A signal for 0.39 fmol/μL insulin was detected in the CHCA solution mixed with 0.1 μg/μL Tf (Fig. 2), whereas the signal for 1.6 fmol/μL insulin was not detected in the CHCA solution mixed with 1.0 μg/μL Tf (data not shown). These results suggest that the detection limit was also decreased in the presence of a high concentration of Tf.

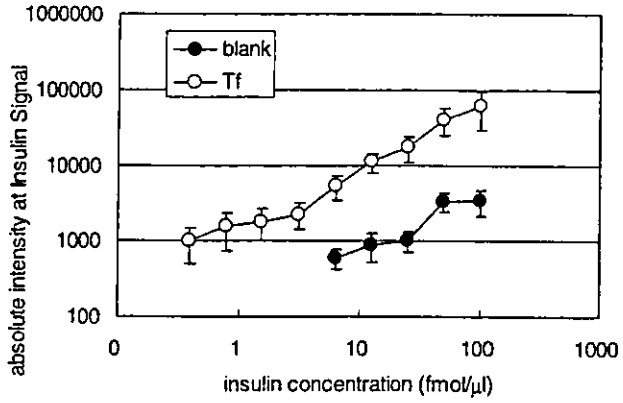

Figure 2. Dependence of insulin signals on insulin concentration. Sequentially diluted human insulin solution (100 to 0.20 fmol/μL in deionized water) and matrix solution were mixed in equal volumes. The matrix solution was a 5:1 mixture of the CHCA solution with either deionized water or Tf solution (0.10 μg/μL). The absolute intensity of the insulin signal obtained from Tf-mixed CHCA (open circles) is compared with that obtained for the control CHCA (closed circles). Each point represents the mean ± S.E. of four tests.

It is known that an excess amount of protein components can strongly influence the behavior of the MALDI process, resulting in partial or complete ion signal suppression.[24] In addition, the optimum mass ratio between the analyte and matrix for MALDI analysis has been demonstrated empirically.[15] When the CHCA was mixed with 1.0 μg/μL Tf, the excess amount of Tf might have suppressed the signal intensity of insulin as well. However, if that amount is appropriate, Tf appears somehow capable of enhancing the signal.

To determine whether or not the enhancement of the insulin MALDI-TOFMS signal intensity was specific to Tf, the CHCA solution was mixed with serially diluted solutions of several peptides and proteins before its addition to the insulin solution. The insulin signal intensity was also enhanced in the presence of ferritin (20 kDa), BSA (66 kDa), or IgG (150 kDa) (Fig. 4(a)). However, this was not found to occur in a simple concentration-dependent manner in the case of either ferritin or IgG; furthermore, when the CHCA solution was mixed with more than 2.0 μg/μL of these protein solutions, no insulin signal was detected. The enhancement of the insulin signal intensity was relatively small in the presence of peptides such as hANP (3.1 kDa) and glucagon (3.4 kDa). In addition, when the CHCA solution was mixed with more than 77 ng/μL of hANP or 87 ng/μL of glucagon, no insulin signal was detected. Among the tested peptides and proteins, the insulin signal intensity was enhanced most effectively in the presence of Tf (80 kDa) or BSA. Therefore, it is probable that this type of enhancement requires an added protein of moderate molecular weight, namely 66–80 kDa.

With regard to the results for the serial dilutions of the added peptides and proteins, the highest S/N values were obtained at 4.8 ng/μL hANP, 5.4 ng/μL glucagon, 66 ng/μL ferritin, 0.13 μg/μL BSA, 0.13 μg/μL Tf, or 0.57 μg/μL

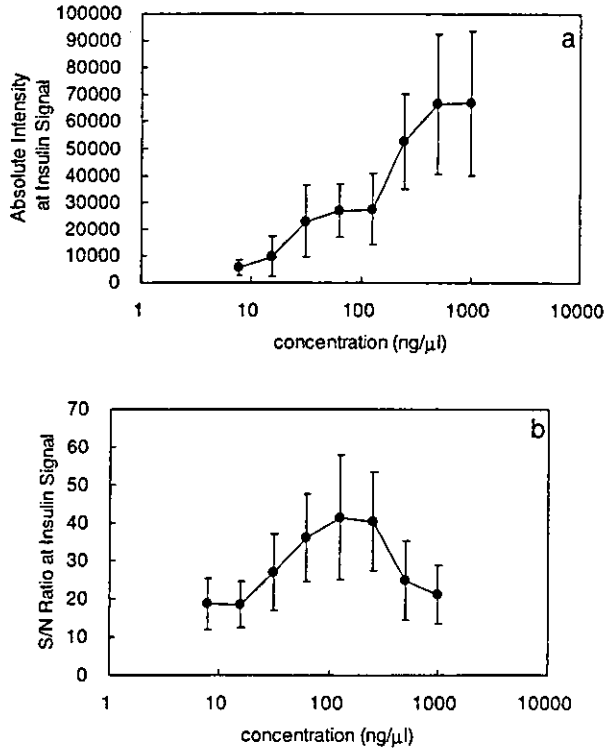

Figure 3. Dependence of insulin signal on Tf concentration. Serially diluted Tf solution was added to five volumes of the CHCA solution before mixing the resulting solution with an equal volume of human insulin (100 fmol/μL): (a) absolute intensity (arbitrary units) and (b) S/N ratio of the insulin signal in the MALDI analysis. Each point represents the mean ± S.E. of four tests.

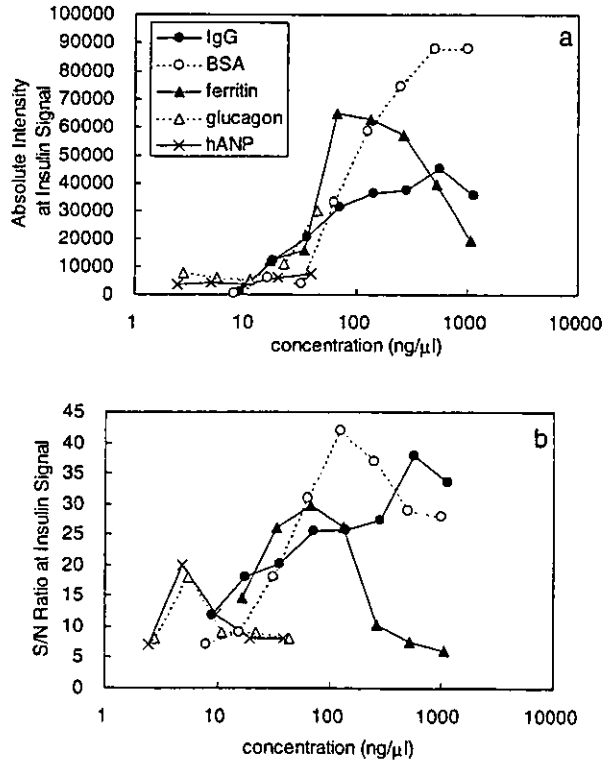

Figure 4. Dependence of insulin signal on concentrations of various added proteins. Serially diluted IgG, BSA, ferritin, glucagon, or hANP solution was added to the CHCA solution before the solution was mixed with the human insulin solution (100 fmol/μL): (a) absolute intensity (units) and (b) S/N ratio of the insulin signal. Each point represents the average of duplicate samples.

IgG (Figs. 3(b) and 4(b)), which correspond to 0.26 pmol, 0.26 pmol, 0.50 pmol, 0.32 pmol, 0.26 pmol, and 0.62 pmol, respectively, in each well. Thus, the optimum molar concentrations occurred in the same scale order, although the optimum mass concentrations of polypeptides required to enhance the signal differed markedly between the proteins and small peptides. In addition, the molar concentrations of excess peptides or proteins required to suppress the insulin signal were also found to exhibit the same scale in the same order. The ionization of insulin appeared to depend on the molar concentration of the peptide or protein which was mixed with the CHCA matrix solution.

To examine whether or not the signal enhancement was specific to human insulin, the CHCA solution premixed with Tf or BSA (0.10 μg/μL) was added to a solution of peptides and proteins, which included hANP, glucagon, human insulin, IGF-I, and ProteoMass Peptide & Protein at concentrations of 50 fmol/μL each. The signal intensities of [angiotensin II]$^+$ (1046 Da), [synthetic peptide $P_{14}R$]$^+$ (1534 Da), and [ACTH fragment]$^+$ (2465 Da) were either not enhanced or were reduced in the matrix premixed with Tf or BSA (Table 1). However, the signal intensities of [hANP]$^+$ (3080 Da), [glucagon]$^+$ (3483 Da), [insulin B chain]$^+$ (3494 Da), and [bovine insulin]$^+$ (5730 Da) were enhanced as well as that of [human insulin]$^+$ (5808 Da) (Table 1, Fig. 5). The signal intensities of [IGF-I]$^+$ (7649 Da), [cytochrome C]$^+$ (12 362 Da), and [cytochrome C]$^{2+}$ were enhanced more than that of human insulin in the presence of Tf or BSA. In addition, the signals of [apomyoglobin]$^+$ (16 952 Da) and [apomyoglobin]$^{2+}$ were clearly observed in the presence of Tf or BSA, although their signals were not detected in the control matrix. In this latter case, the signal of [apomyoglobin]$^+$ overlapped with that of BSA, but not of Tf; therefore, it was more advantageous to use Tf than BSA for detecting this signal. Since BSA was included in the ProteoMass Peptide & Protein solution, the signals of [BSA]$^+$ (66 430 Da), [BSA]$^{2+}$, [BSA]$^{3+}$, and [BSA]$^{4+}$ were also detected in the presence of Tf (Table 1, Fig. 5(b)).

The results reported above demonstrate that the enhancement of the signal intensity achieved with the use of Tf and BSA was observed for both peptides and proteins, and this effect was not specific to human insulin. The degree of enhancement was dependent on the molecular weights of the peptides and proteins, and no such enhancement was observed in the case of small peptides; in this regard a dividing line appeared to exist between [ACTH fragment]$^+$ (2465 Da) and [hANP]$^+$ (3080 Da).

The mechanism by which signal intensity enhancement was achieved with the use of peptides and proteins mixed with the matrix solution remains unclear. However, when super DHB (a co-matrix of DHB and 2-hydroxy-5-methoxybenzoic acid) was used as the matrix, ion yields and S/N ratio improved, especially for the high-mass range.[20] It has been suggested that this signal enhancement was caused by a disorder in the DHB lattice, allowing 'softer' desorption. This type of signal enhancement has also been observed in the case of substance P in CHCA after fast evaporation of an acetone solvent, which resulted in the more homogeneous distribution of matrix and analytes.[18] In addition, better mass resolution has been observed in the spectra of cytochrome C in a CHCA matrix desorbed from polyethylene and polypropylene membranes than has been observed with a CHCA matrix desorbed from stainless steel; it was thus suggested that such improved resolution might be due at least in part to the formation of relatively small matrix crystals within the membrane lattice structure.[25] In the present study, Tf and other proteins might have led to a similar disorganization in the CHCA lattice, resulting in the homogeneous distribution of insulin in the CHCA. However, the mechanism may differ from that suggested here, since the disorder in the CHCA lattice cannot reasonably account for why both Tf and BSA were able to enhance the insulin signal more effectively than either hANP or glucagon. As the next step, we are now planning to compare the crystals of the additive macromolecules plus matrix with those of the control matrix, using microscopic examination, to help elucidate the enhancement mechanism. We also intend to investigate whether the enhancement effect is observed in matrices other than CHCA. If crystallization is important,

Table 1. Signal intensities for proteins and peptides obtained using a matrix premixed with deionized water or with solutions of Tf or BSA

	Water	Tf	BSA
[Angiotensin II]$^+$	27 834 ± 10 757	17 057 ± 5021	19 755 ± 11 237
[P14R]$^+$	41 689 ± 15 289	30 675 ± 8588	29 237 ± 13 330
[ACTH 18–39]$^+$	4371 ± 1586	3801 ± 2246	5458 ± 3826
[hNAP]$^+$	5158 ± 1323	6889 ± 2879	9523 ± 6384
[human glucagon]$^+$	435 ± 183	674 ± 324	978 ± 566
[insulin B chain]$^+$	367 ± 257	997 ± 251	715 ± 479
[bovine insulin]$^+$	639 ± 100	6266 ± 2736	7498 ± 5331
[human insulin]$^+$	1267 ± 130	13 321 ± 5057	12 982 ± 6863
[equine cytochrome C]$^{2+}$	166 ± 83	5668 ± 1975	3460 ± 1442
[human IGF-I]$^+$	459 ± 81	7667 ± 1808	6263 ± 2872
[equine apomyoglobin]$^{2+}$	nd	2249 ± 994	2217 ± 1087
[equine cytochrome C]$^+$	114 ± 43	7629 ± 1804	4006 ± 1981
[BSA]$^{4+}$	nd	52 ± 14	2459 ± 604
[equine apomyoglobin]$^+$	nd	1347 ± 700	2090 ± 1316
[BSA]$^{3+}$	nd	155 ± 13	3721 ± 1426
[BSA]$^{2+}$	nd	114 ± 27	3624 ± 1681
[BSA]$^+$	nd	25 ± 8	634 ± 433

Each entry is the average of the most intense signals from four samples. nd: no signal was detected.

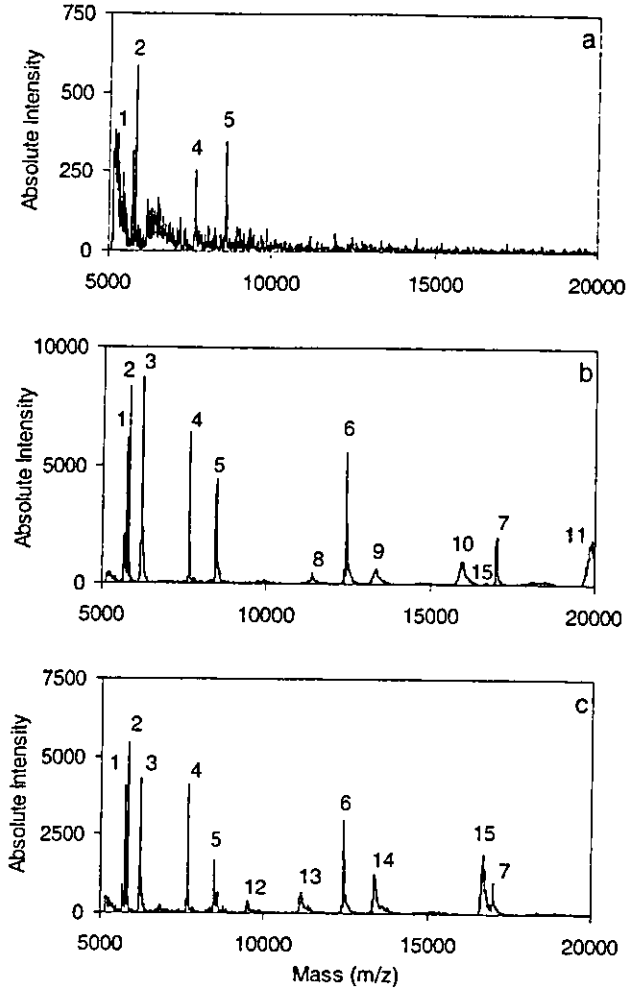

Figure 5. MALDI mass spectra of a mixture of peptides and proteins. The mixture of peptides and proteins (50 fmol/μL each) and the matrix solution were mixed together in equal volumes. The matrix solution was a 5:1 mixture of the CHCA solution with (a) deionized water; (b) Tf solution (0.10 μg/μL); and (c) BSA solution (0.10 μg/μL). Signal 1, [bovine insulin]$^{+}$ (5730 Da); 2, [human insulin]$^{+}$ (5808 Da); 3, [cytochrome C]$^{2+}$; 4, [IGF-I]$^{+}$ (7649 Da); 5, [apomyoglobin]$^{2+}$; 6, [cytochrome C]$^{+}$ (12 362 Da); 7, [apomyoglobin]$^{+}$ (16 952 Da); 8, [Tf]$^{7+}$; 9, [Tf]$^{6+}$; 10, [Tf]$^{5+}$; 11, [Tf]$^{4+}$; 12, [BSA]$^{7+}$; 13, [BSA]$^{6+}$; 14, [BSA]$^{5+}$; and 15, [BSA]$^{4+}$.

the effect should not be observed when using liquid matrices.[26,27]

The present results suggest that the enhancement brought about by either Tf or BSA could be applicable to the improvement of sensitivity in the detection of proteins by MALDI-TOFMS in general. However, when Tf or BSA was used as an enhancer in a MALDI-TOFMS system, signals from Tf and BSA were also detected, which sometimes interfered with the analysis of the target proteins. Therefore, neither Tf nor BSA appears to be the best possible enhancer. Further studies are currently underway in order to discover the best macromolecule as an enhancer.

CONCLUSIONS

We have demonstrated that the signal intensities of insulin and of several peptides and proteins were enhanced in CHCA premixed with Tf or other peptides or proteins. The characteristics of this type of enhancement are as follows: (1) Tf (80 kDa) and BSA (66 kDa) led to better signal enhancement than did small peptides and proteins (<20 kDa) or IgG (150 kDa); (2) the optimum S/N value was observed when the added amount of peptide or protein was within the range 0.26–0.62 pmol; and (3) the signals of peptides of high molecular weight (>3000 Da) were enhanced by the addition of Tf or BSA to CHCA, although the signals of small peptides (<2500 Da) were not enhanced. This type of enhancement may be useful for the improvement of protein analyses with MALDI-TOFMS.

Acknowledgements

This study was supported in part by a research grant on Human Genome, Tissue Engineering Food Biotechnology from the Ministry of Health, Labor and Welfare, Japan.

REFERENCES

1. Roberts GD, Johnson WP, Burman S, Anumula KR, Carr SA. *Anal. Chem.* 1995; **67**: 3613.
2. Gygi SP, Rist B, Gerber SA, Turecek F, Gelb MH, Aebersold R. *Nat. Biotechnol.* 1999; **17**: 994.
3. Münchbach M, Quadroni M, Miotto G, James P. *Anal. Chem.* 2000; **72**: 4047.
4. Yao X, Freas A, Ramirez J, Demirev PA, Fenselau C. *Anal. Chem.* 2001; **73**: 2836.
5. Cagney G, Emili A. *Nat. Biotechnol.* 2002; **20**: 163.
6. Vogt JA, Schroer K, Hözler K, Hunzinger C, Klemm M, Biefang-Arndt K, Schillo S, Cahill MA, Schlattenholz A, Matthies H, Stegmann W. *Rapid Commun. Mass Spectrom.* 2003; **17**: 1273.
7. Kuyama H, Watanabe M, Toda C, Ando E, Tanaka K, Nishimura O. *Rapid Commun. Mass Spectrom.* 2003; **17**: 1642.
8. Wu SL, Choudhary G, Ramström M, Bergquist J, Hancock WS. *J. Proteome Res.* 2003; **2**: 383.
9. Nakanishi T, Okamoto N, Tanaka K, Shimizu A. *Biol. Mass Spectrom.* 1994; **23**: 230.
10. Nelson RW, Krone JR, Bieber AL, Williams P. *Anal. Chem.* 1995; **67**: 1153.
11. Tubbs KA, Nedelkov D, Nelson RW. *Anal. Biochem.* 2001; **289**: 26.
12. Tanaka K, Waki H, Ido Y, Akita S, Yoshida Y, Yoshida T. *Rapid Commun. Mass Spectrom.* 1988; **2**: 151.
13. Karas M, Hillenkamp F. *Anal. Chem.* 1988; **60**: 2299.
14. Beavis RC, Chait BT. *Anal. Chem.* 1990; **62**: 1836.
15. Strupat K, Karas M, Hillenkamp F. *Int. J. Mass Spectrom. Ion Processes* 1991; **111**: 89.
16. Beavis RC, Chaudhary T, Chait BT. *Org. Mass Spectrom.* 1992; **27**: 156.
17. Vorm O, Roepstorff P, Mann M. *Anal. Chem.* 1994; **66**: 3281.
18. Köstler C, Castoro JA, Wilkins CL. *J. Am. Chem. Soc.* 1992; **114**: 7572.
19. Billeci TM, Stults JT. *Anal. Chem.* 1993; **65**: 1709.
20. Karas M, Ehring H, Nordhoff E, Stahl B, Strupat K, Hillenkamp F, Grehl M, Krebs B. *Org. Mass Spectrom.* 1993; **28**: 1476.
21. Tsarbopoulos A, Karas M, Strupat K, Pramanik BN, Nagabhushan TL, Hillenkamp F. *Anal. Chem.* 1994; **66**: 2062.
22. Yuan X, Desiderio DM. *J. Mass Spectrom.* 2002; **37**: 512.
23. Botting CH. *Rapid Commun. Mass Spectrom.* 2003; **17**: 598.
24. Nelson RW, McLean MA. *Anal. Chem.* 1994; **66**: 1408.
25. Worrall TA, Cotter RJ, Woods AS. *Anal. Chem.* 1998; **70**: 750.
26. Carda-Broch S, Berthod A, Armstrong DW. *Rapid Commun. Mass Spectrom.* 2003; **17**: 553.
27. Turney K, Harrison WW. *Rapid Commun. Mass Spectrom.* 2004; **18**: 629.

Enhancement of Hepatocyte Growth Factor-Induced Cell Scattering in *N*-Acetylglucosaminyltransferase III-transfected HepG2 Cells

Masashi HYUGA,* Sumiko HYUGA, Nana KAWASAKI, Miyako OHTA, Satsuki ITOH, Shingo NIIMI, Toru KAWANISHI, and Takao HAYAKAWA

Division of Biological Chemistry and Biologicals, National Institute of Health Sciences; 1–18–1 Kamiyoga, Setagaya-ku, Tokyo 158–8501, Japan. Received January 9, 2004; accepted March 29, 2004; published online April 1, 2004

N-Acetylglucosaminyltransferase III (GnT-III), which catalyzes the synthesis of a bisecting GlcNAc residue of *N*-glycans, is thought to be involved in the function of glycoproteins such as growth factor receptors. We investigated the effects of the overexpression of GnT-III on the hepatocyte growth factor (HGF) receptor c-Met, a glycoprotein, in human hepatocarcinoma HepG2 cells. GnT-III activity was elevated about 250-fold in HepG2 cells stably transfected with the GnT-III gene, whereas no significant change in GnT-III activity was observed in mock transfectants. Cell scattering assay revealed that HGF-induced cell scattering was enhanced depending on the GnT-III activities in the GnT-III transfectants. Western blot analysis and E-PHA lectin blot analysis showed that the level of c-Met protein was the same in both transfectants; however, the bisecting GlcNAc residue on c-Met was detected only in the GnT-III transfectants. Although the peak level of c-Met phosphorylation was not different in both transfectants, the level of tyrosine phosphorylation of c-Met decreased more rapidly in the GnT-III transfectants than in the mock transfectants. Furthermore, HGF-induced extracellular-regulated kinase (ERK) phosphorylation was slightly higher in the GnT-III transfectants than in the mock transfectants. These results show that overexpression of GnT-III in HepG2 cells enhances HGF-induced cell scattering, which may result from, at least in part, enhancement of HGF-induced ERK phosphorylation.

Key words *N*-acetylglucosaminyltransferase III; cell scattering; hepatocyte growth factor; c-Met; extracellular-regulated kinase (ERK)

N-Acetylglucosaminyltransferase III (GnT-III: EC 2.4.1.144) is one of the glycosyltranferases and catalyzes the synthesis of a bisecting GlcNAc residue to the β-mannoside of the trimannose core in *N*-glycans.[1] After introduction of the bisecting GlcNAc residue to the biantennary sugar chain, further processing and elongation of *N*-glycans by the other glycosyltransferases are suppressed,[2—4] resulting in alterations of structure with reduction of size. It seems that GnT-III may affect the functions of various glycoproteins. In this respect, it is noteworthy that the overexpression of GnT-III affects receptor tyrosine kinases such as the epidermal growth factor (EGF) and NGF receptor Trk, followed by the modulation of signal transductions.[5] EGF inhibits the growth of U373 MG glioma cells, while the overexpression of GnT-III causes the decreased binding of EGF to its receptor and then autophosphorylation of the receptor, resulting in the increase in the cell growth rate.[6] In contrast, the overexpression of GnT-III in HeLaS3 cells does not affect EGF receptor autophosphorylation, but enhances internalization of the receptors, resulting in the increase of the EGF-induced phosphorylation of extracellular-regulated kinase (ERK).[7] In PC 12 cells, nerve growth factor-stimulated Trk receptor autophosphorylation and signal transduction was disrupted by the overexpression of GnT-III.[8] This evidence suggests that GnT-III may also affect the other growth factors-induced signal transduction by the modulation of the function of their receptors in some ways.

Since the expression of GnT-III is associated with many physiological and pathological processes in the liver, including its regeneration[9] and hepatocarcinogenesis,[10] it is assumed that GnT-III is involved in the processes via the modulation of some glycoproteins such as the receptor of the hepatocyte growth factor (HGF), c-Met. In the present study, we investigated the effects of the overexpression of GnT-III on the scattering of human hepatocarcinoma HepG2 cells, a defined HGF-induced biological response.

MATERIALS AND METHODS

Materials The recombinant human HGF was purchased from R&D systems (Minneapolis, MN, U.S.A.). The Dulbecco's modified Eagle's medium (DMEM), fetal calf serum (FCS), ampicillin, G418, Lipofectamine plus, and Opti-MEM were purchased from Life Technologies Inc. (Rockville, MD, U.S.A.). The human brain cDNA was purchased from Origene Technologies Inc. (Rockville, MD, U.S.A.). The mammalian expression vector pCI-neo was purchased from Promega (Madison, WI, U.S.A.). The protease inhibitors cocktail was purchased from Sigma Chemical Co (St. Louis, MO, U.S.A.). The PVDF membrane was purchased from Millipore Corporation (Bedford, MA, U.S.A.). Biotinylated E-PHA was purchased from Vector Laboratories (Burlingame, CA, U.S.A.). Protein G-immobilized magnetic beads (BioMag Protein G) were purchased from Polysciences, Inc. (Warrington, PA, U.S.A.). The anti-human c-Met antibody (C-23), anti-phospho-ERK antibody (E-4) and anti-ERK antibody (K-23) were purchased from Santa Cruz Biotechnology, Inc. (Santa Cruz, CA, U.S.A.). The monoclonal anti-phosphotyrosine antibody (PY20) was purchased from Transduction Laboratories (Lexington, KY, U.S.A.). The biotinylated anti-mouse IgG antibody, biotinylated anti-rabbit IgG antibody, peroxidase-conjugated rabbit anti-mouse IgG, and ECL chemiluminescence detection kit were purchased from Amersham-Pharmacia Biotech (Piscataway, NJ, U.S.A.). The vectastain ABC kit was purchased from Vector Laboratories (Burlingame, CA, U.S.A.). All other chemicals were obtained from commercial sources, and were of the highest purity available.

* To whom correspondence should be addressed. e-mail: mhyuga@nihs.go.jp

Cell Culture Human hepatocarcinoma HepG2 cells were obtained from the Japanese Cancer Research Resources Bank (Tokyo, Japan). The HepG2 cells and GnT-III gene transfectants were cultured in DMEM supplemented with 10% FCS and 0.1 mg/ml of ampicillin under a humidified atmosphere of 95% air and 5% CO_2. Following incubation for 1 d with serum-free DMEM, the cells were incubated with 50 ng/ml of HGF in serum-free DMEM.

Expression Vector Construct, Gene Transfection, and Selection of Cells The human GnT-III cDNA was amplified by PCR using human brain cDNA as a template. The cDNA fragment containing the entire coding sequence was inserted into the pCI-neo *EcoR* I site and the final construct, pCI-GnT-III, was obtained. The pCI-neo is a mammalian expression vector which includes the cytomegalovirus enhancer/promoter and the G418-resistant gene. HepG2 cells were plated in a 6-cm plastic culture dish at a density of 1×10^6 cells/ml. After 24 h, the cells were washed twice with ice-cold phosphate-buffered saline (PBS), pH 7.2, and the medium was changed to serum-free Opti-MEM. The pCI-GnT-III vector or pCI-neo vector (20 μg) was mixed with Lipofectamine plus, 100 μl of which was added to the HepG2 cells. After 5 h incubation, the medium was changed to DMEM supplemented with 10% FCS. Stable transfectants were selected using 1 mg/ml G418.

GnT-III Activity The GnT-III activity was measured according to the methods described previously.[11] Briefly, cell pellets were homogenized in ice-cold PBS containing protease inhibitors, and the supernatant was obtained after removal of the nucleus fraction by centrifugation for 20 min at $900\times g$. The GnT-III activity in the supernatant was assayed by high performance liquid chromatography methods using the fluorescence-labeled sugar chain (GlcNAcβ-1, 2-Manα-1, 6-[GlcNAcβ-1, 2-Manα-1, 3-] Manβ-1, 4-GlcNAcβ-1, 4-GlcNAc-pyridylamino) as a substrate. The substrate was prepared according to the method of Tokugawa *et al.*[12]

Cell Scattering Assay The HepG2 cells were plated in a 6-cm plastic culture dish at a density of 5×10^4 cells/ml. The HepG2 cells were allowed to grow as discrete colonies for 2—3 d. The culture medium was then replaced with fresh DMEM medium containing 50 ng/ml HGF. After 24 h, the cells were observed under a phase contrast microscope.

Immunoprecipitation and Western Blot Analysis The cultured cells were washed twice with ice-cold PBS and disrupted in the lysis buffer (20 mM Tris, pH 7.2, 1% Triton X-100, 10% glycerol, 1 mM APMSF, 5 mM aprotinin, 1 mM sodium orthovanadate, 10 mM sodium fluoride, and 10 mM iodoacetamide). The protein concentrations were determined using a protein assay kit (Bio-Rad, CA, U.S.A.). The cell-free lysates (1 mg) were immunoprecipitated with the anti-human c-Met antibody and protein G-immobilized magnetic beads (BioMag Protein G). For Western blot analysis, whole cell lysates or immunoprecipitates were subjected to 6 or 10% sodium dodecyl sulfate–polyacrylamide gel electrophoresis (SDS-PAGE) under reducing conditions, and then transferred to a PVDF membrane. The blot was blocked with 1% bovine serum albumin (BSA) in Tris-buffered saline containing 0.1% Tween 20 (TBST). For the detection of c-Met, the blot was incubated with anti-human c-Met antibody, and biotinylated anti-rabbit IgG antibody. For the detection of the phosphorylated tyrosine residues of c-Met, the blot was incubated with a monoclonal anti-phosphotyrosine antibody, and peroxidase-conjugated rabbit anti-mouse IgG. For the detection of phosphorylated ERK1/2, the blot was incubated with anti-ERK antibody, and biotinylated anti-mouse IgG antibody. Biotinylated antibody was detected using a Vectastain ABC-kit, and the blots were developed using the ECL chemiluminescence detection kit according to the manufacturer's instructions.

Lectin Blot Analysis Immunoprecipitated c-Met were subjected to 6% SDS-PAGE and transferred to PVDF membranes, as described above. The blot was blocked with 1% BSA in TBST and then incubated with 1 μg/ml biotinylated erythroagglutinating phytohemagglutinin (E-PHA) in TBST for 1 h at room temperature. After washing with TBST, the lectin-reactive proteins were detected using a Vectastain ABC kit and the ECL chemiluminescence detection kit.

RESULTS

Establishment of HepG2 Cell Lines Stably Expressing GnT-III The GnT-III expression vector pCI-GnT-III was transfected into the HepG2 cells. The G418-resistant cells were screened as candidates of the GnT-III transfectants. Two randomly selected G418-resistant clones were evaluated for GnT-III activity. The clones expressing moderately and highly were designated HepG2-IIIm and HepG2-IIIh, respectively. A pCI-neo vector transfectant, designated as HepG2-mock, was also established as a negative control. The GnT-III activity in the HepG2-IIIm and HepG2-IIIh cells was significantly elevated about 20- and 250-fold, respectively, whereas the activity in the HepG2-mock cells did not differ significantly among the parental HepG2 cells (Table 1).

Enhancement of HGF-Induced Cell Scattering in GnT-III Transfectants To determine the effect of the overexpression of GnT-III on the HGF-induced cell scattering, the GnT-III transfectants and mock transfectants were examined. When the HepG2-mock cells were cultured, they showed a cobble-stone shape and had formed colonies of the cells (Fig. 1A). No significant difference in cell morphology of the GnT-III transfectants was observed (Figs. 1B, C). HepG2-mock cells scattered following cell-cell dissociation by the stimulation with HGF (Fig. 1D). The cell scattering of the GnT-III transfectants was more pronounced than the HepG2-mock cells; the enhancement of cell scattering was most pronounced in the HepG2-IIIh cells that had a high GnT-III activity (Figs. 1E, F).

Analysis of c-Met of GnT-III Transfectants The expression levels of the c-Met protein in GnT-III transfectants were analyzed by Western blot analysis. No significant change of the level of c-Met was observed (Fig. 2). To analyze the alterations of the *N*-glycan structure on c-Met, E-

Table 1. Enzyme Activities of GnT-III in Mock- and GnT-III Transfected HepG2 Cells

Cell line	GnT-III activity [pmol/h/mg protein]
HepG2	79±30
HepG2-mock	149±50
HepG2-IIIm	1400±260
HepG2-IIIh	19600±1350

Data were mean±S.E. of three separate experiments.

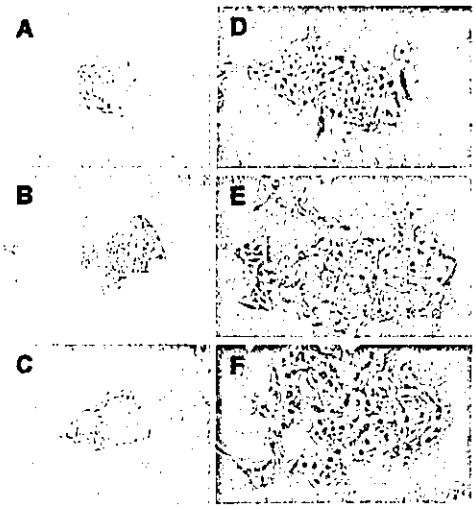

Fig. 1. HGF-Induced Cell Scattering in HepG2-Mock Cells and GnT-III Transfected HepG2 Cells

HepG2 mock-cells (A, D), HepG2-IIIm cells (B, E), and HepG2-IIIh cells (C, F) were cultured with (D, E, F) or without (A, B, C) HGF (50 ng/ml) for 24 h. Representative fields were photographed using a phase-contrast microscope.

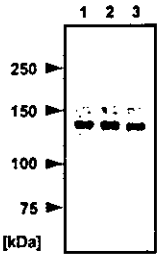

Fig. 2. Western Blot Analysis of c-Met

Total cell lysates from HepG2-mock cells (lane 1), HepG2-IIIm cells (lane 2), and HepG2-IIIh cells (lane 3) were subjected to 6% SDS-PAGE and then transferred to PVDF membrane. The blots were probed with anti-c-Met antibody.

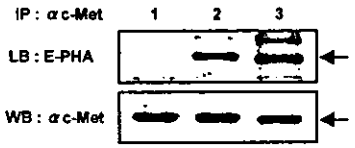

Fig. 3. Lectin Blot Analysis of c-Met

C-Met was immunoprecipitated from cell lysates of HepG2-mock cells (lane 1), HepG2-IIIm cells (lane 2), and HepG2-IIIh cells (lane 3). Immunoprecipitates were subjected to 6% SDS-PAGE and then transferred to PVDF membrane. The blots were probed with E-PHA (upper panel) or anti-c-Met antibody (lower panel). Arrows indicate c-Met.

PHA lectin blot analysis was performed. E-PHA binds specifically to bisecting GlcNAc residues.[13] Immunoprecipitated c-Met from the HepG2-IIIm cells and the HepG2-IIIh cells showed significant reactivity of E-PHA (Fig. 3), showing that *N*-glycan on c-Met was modified with bisecting GlcNAc residues. It was noted that the apparent molecular size of c-Met from the HepG2-IIIh cells were smaller than that from the HepG2-mock cells. The following experiments were performed with HepG2-IIIh cells and HepG2-mock cells.

Tyrosine Phosphorylation of c-Met in Gn T-III Transfectants To determine the effect of the GnT-III transfection on HGF signaling, HGF-induced tyrosine phosphorylation of

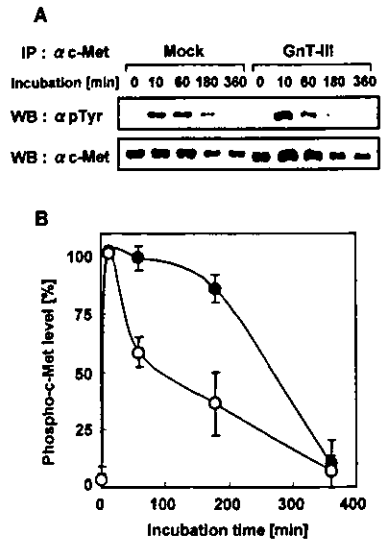

Fig. 4. The Time Course of the Tyrosine Phosphorylation of c-Met

(A) Cells were harvested at the indicated time after HGF treatment (50 ng/ml). C-Met, immunoprecipitated from the cell lysates of HepG2-mock cells (●) and HepG2-IIIh cells (○) were subjected to 6% SDS-PAGE and then transferred to a PVDF membrane. The blot was probed with anti-phosphotyrosine antibody (upper panel) or anti-human c-Met antibody (lower panel). One representative result of three separate experiments is shown. (B) The intensities of the bands obtained with phosphorylated c-Met were normalized to the intensities of the c-Met bands. These values are shown as percentages of the level of c-Met phosphorylation in HepG2-mock cells treated with HGF for 10 min (mean±S.E., three separate experiments).

c-Met in HepG2-IIIh cells and HepG2-mock cells were examined. The c-Met phosphorylation level reached a peak by 10 min after the HGF treatment in each transfectant. Although no difference in the peak level of c-Met phosphorylation between the HepG2-IIIh cells and HepG2-mock cells was observed, the level of c-Met phosphorylation in the HepG2-IIIh cells was reduced more rapidly than in the HepG2-mock cells (Fig. 4).

ERK Activation in GnT-III Transfectants To further clarify the effect of the GnT-III transfection on HGF signaling, the HGF-induced phosphorylation of ERK in the HepG2-IIIh cells and HepG2-mock cells was also examined. The time course of the tyrosine phosphorylation of ERK showed that the phosphorylated ERK level reached a peak by 10 min after treatment in each transfectant. The peak level in the HepG2-IIIh cells was slightly higher than in the HepG2-mock cells (Fig. 5).

DISCUSSION

In this paper we investigated the effects of the overexpression of GnT-III on the scattering of human hepatocarcinoma HepG2 cells, a defined HGF-induced biological response, since the function of the HGF receptor c-Met could be modulated by GnT-III transfection followed by the alteration of its biological functions, as described in the "INTRODUCTION" section. The results showed that GnT-III gene transfection increases GnT-III activity by about 250 fold, followed by a significant increase of E-PHA reactivity with c-Met (Fig. 3), indicating that the transfection of GnT-III increased the amount of bisecting oligosaccharide residue on c-Met. In addition, the molecular size of c-Met in the HepG2-IIIh cells was smaller than that in the HepG2-mock cells (Figs. 2, 3), suggesting that an elongation of *N*-glycans on c-Met was

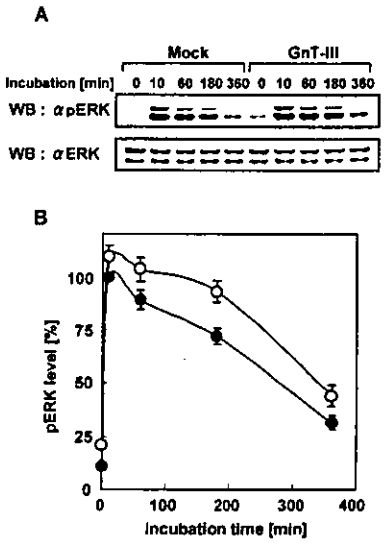

Fig. 5. The Time-Course of the Tyrosine Phosphorylation of ERK

(A) Cells were stimulated with 50 ng/ml HGF and harvested at the indicated times. Whole cell lysates of HepG2-mock cells (●) and HepG2-IIIh cells (○) were subjected to 10% SDS-PAGE and then transferred to a PVDF membrane. The blot was probed with anti-phospho-ERK antibody (upper panel) or anti-ERK antibody (lower panel). One representative result of three separate experiments is shown. (B) The intensities of the bands obtained with phospho-ERK were normalized to the intensities of the ERK bands. These values are shown as percentages of the level of ERK phosphorylation in HepG2-mock cells treated with HGF for 10 min (mean±S.E., three separate experiments).

suppressed by the bisecting GlcNAc residue. The same observation has been shown in various glycoproteins such as the EGF receptor,[7] E-cadherin,[14,15] and CD44.[16]

We investigated the effect of the overexpression of GnT-III on HGF-induced cell scattering using these transfectants, because cell scattering is one of the HGF-induced biological responses and an important component of several physiological and pathological processes. We found that HGF-induced cell scattering in the GnT-III transfectants was enhanced depending on the GnT-III activities. As far as we know, this is the first report of the enhancing effect of HGF-induced cell scattering by the overexpression of GnT-III.

To confirm the effect of GnT-III overexpression on HGF signaling, we first investigated the effect on the HGF-induced tyrosine phosphorylation of c-Met in GnT-III transfectants. Unexpectedly, the peak level of the tyrosine phosphorylation of c-Met did not change by GnT-III. In addition, the level of c-Met phosphorylation was reduced quite a bit more rapidly than that in the HepG2-mock cells. Previous studies shown that HGF stimulation also leads to down-regulation of the receptor.[17] We assume that the rapid dephosphorylation was caused by up-regulated HGF signaling.

We further examined the effects on the HGF-induced phosphorylation of ERK, because ERK activation is associated with HGF-induced cell scattering.[18] The ERK phosphorylation was slightly enhanced by the GnT-III overexpression, showing that the enhancement of cell scattering involves the up-regulation of the HGF-induced ERK phosphorylation. The mechanisms by which GnT-III overexpression affects ERK activation is now under investigation. It has been shown that GnT-III overexpression enhances the EGF-induced ERK phosphorylation in HelaS3 cells by up-regulation of the internalization rate of the receptors.[7] A possible mechanism by which GnT-III overexpression enhances HGF-induced ERK phosphorylation is that GnT-III affects c-Met internalization.

In this study, we demonstrated that GnT-III overexpression increased the amount of bisecting oligosaccharide structures and shortened the *N*-glycans associated with c-Met. Lectin blot analysis of total showed that *N*-glycans of the other glycoproteins were also changed by GnT-III overexpression (data not shown). Therefore, the glycoproteins involved in cell scattering, such as E-cadherin and integrin, are candidate proteins for involvement in the enhancement of cell scattering by GnT-III overexpression. In fact, it has been reported that GnT-III overexpression affects their biological functions.[14,15,19] Further study is needed to clarify the mechanism involved in the enhancement of cell scattering.

In evaluating the significance of the present results, it seems worthwhile to examine the relation of the change of GnT-III with the action of HGF *in vivo*. In the normal rat liver, GnT-III activity is very low. However, the activity increased about 4-fold in regenerating rat liver.[9] HGF is induced in regenerating rat liver, and stimulates hepatocyte growth. In addition, it was shown that hepatocarcinoma exhibited a high level of GnT-III activity, whereas normal liver contains very little.[20] Autocrine HGF signaling leads to abnormal malignant progression.[21] Therefore, the increase of GnT-III may contribute to liver regeneration and hepatocarcinoma progression by the enhanced HGF signal.

In conclusion, we demonstrated that the overexpression of GnT-III caused the enhancement of HGF-induced cell scattering, and suggest that the enhancement of cell scattering involves, at least in part, enhancement of the HGF-induced ERK phosphorylation.

Acknowledgments This work was supported by a grant-in-aid for research on health sciences focusing on drug innovation from the Japan Health Sciences Foundation.

REFERENCES

1) Nishikawa A., Ihara Y., Hatakeyama M., Kangawa K., Taniguchi N., *J. Biol. Chem.*, **267**, 18199—18204 (1992).
2) Easton E. W., Bolscher J. G., van den Eijnden D. H., *J. Biol. Chem.*, **266**, 21674—21680 (1991).
3) Gu J., Nishikawa A., Tsuruoka N., Ohno M., Yamaguchi N., Kangawa K., Taniguchi N., *J. Biochem.* (Tokyo), **113**, 614—619 (1993).
4) Sasai K., Ikeda Y., Eguchi H., Tsuda T., Honke K., Taniguchi N., *FEBS Lett.*, **522**, 151—155 (2002).
5) Stanley P., *Biochim. Biophys. Acta*, **1573**, 363—368 (2002).
6) Rebbaa A., Yamamoto H., Saito T., Meuillet E., Kim P., Kersey D. S., Bremer E. G., Taniguchi N., Moskal J. R., *J. Biol. Chem.*, **272**, 9275—9279 (1997).
7) Sato Y., Takahashi M., Shibukawa Y., Jain S. K., Hamaoka R., Miyagawa J., Yaginuma Y., Honke K., Ishikawa M., Taniguchi N., *J. Biol. Chem.*, **276**, 11956—11962 (2001).
8) Ihara Y., Sakamoto Y., Mihara M., Shimizu K., Taniguchi N., *J. Biol. Chem.*, **272**, 9629—9634 (1997).
9) Miyoshi E., Ihara Y., Nishikawa A., Saito H., Uozumi N., Hayashi N., Fusamoto H., Kamada T., Taniguchi N., *Hepatology*, **22**, 1847—1855 (1995).
10) Miyoshi E., Nishikawa A., Ihara Y., Gu J., Sugiyama T., Hayashi N., Fusamoto H., Kamada T., Taniguchi N., *Cancer Res.*, **53**, 3899—3902 (1993).
11) Nishikawa A., Fujii S., Sugiyama T., Taniguchi N., *Anal. Biochem.*, **170**, 349—354 (1988).
12) Tokugawa K., Oguri S., Takeuchi M., *Glycoconj. J.*, **13**, 53—56 (1996).
13) Yamashita K., Hitoi A., Kobata A., *J. Biol. Chem.*, **258**, 14753—14755

(1983).
14) Yoshimura M., Ihara Y., Matsuzawa Y., Taniguchi N., *J. Biol. Chem.*, **271**, 13811—13815 (1996).
15) Kitada T., Miyoshi E., Noda K., Higashiyama S., Ihara H., Matsuura N., Hayashi N., Kawata S., Matsuzawa Y., Taniguchi N., *J. Biol. Chem.*, **276**, 475—480 (2001).
16) Sheng Y., Yoshimura M., Inoue S., Oritani K., Nishiura T., Yoshida H., Ogawa M., Okajima Y., Matsuzawa Y., Taniguchi N., *Int. J. Cancer*, **73**, 850—858 (1997).
17) Hammond D. E., Carter S., McCullough J., Urbe S., Vande Woude G., Clague M. J., *Mol. Biol. Cell.*, **14**, 1346—1354 (2001).
18) Sipeki S., BanderE., Buday L., Farkas G., Bacsy E., Ways D. K., Farago A., *Cell Signal*, **11**, 885—890 (1999).
19) Isaji T., Gu J., Nishiuchi R., Zhao Y., Takahashi M., Miyoshi E., Honke K., Sekiguchi K., Taniguchi N., *J. Biol. Chem.*, in press (2004).
20) Nishikawa A., Fujii S., Sugiyama T., Hayashi N., Taniguchi N., *Biochem. Biophys. Res. Commun.*, **152**, 107—112 (1988).
21) Vande Woude G. F., Jeffers M., Cortner J., Alvord G., Tsarfaty I., Resau J., *Ciba Found. Symp.*, **212**, 119—130; discussion 130—112, 148—154 (1997).